

Transfer of Motor Learning from a Virtual to Real Task Using EEG Signals  
Resulting from Embodied and Abstract Thoughts

by

Flavio J. K. da Silva

A Dissertation Presented in Partial Fulfillment  
of the Requirements for the Degree  
Doctor of Philosophy

Approved April 2013 by the  
Graduate Supervisory Committee:

Michael McBeath, Chair  
Stephen Helms Tillery  
Thomas Sugar  
Clark Presson

ARIZONA STATE UNIVERSITY

May 2013

## ABSTRACT

This research is focused on two separate but related topics. The first uses an electroencephalographic (EEG) brain-computer interface (BCI) to explore the phenomenon of motor learning transfer. The second takes a closer look at the EEG-BCI itself and tests an alternate way of mapping EEG signals into machine commands.

We test whether motor learning transfer is more related to use of shared neural structures between imagery and motor execution or to more generalized cognitive factors. Using an EEG-BCI, we train one group of participants to control the movements of a cursor using embodied motor imagery. A second group is trained to control the cursor using abstract motor imagery. A third control group practices moving the cursor using an arm and finger on a touch screen. We hypothesized that if motor learning transfer is related to the use of shared neural structures then the embodied motor imagery group would show more learning transfer than the abstract imaging group. If, on the other hand, motor learning transfer results from more general cognitive processes, then the abstract motor imagery group should also demonstrate motor learning transfer to the manual performance of the same task.

Our findings support that motor learning transfer is due to the use of shared neural structures between imaging and motor execution of a task. The abstract group showed no motor learning transfer despite being better at EEG-BCI control than the embodied group. The fact that more participants were able to learn EEG-BCI control using abstract imagery suggests that abstract imagery may be more suitable for EEG-BCIs for some disabilities, while embodied imagery may be more suitable for others.

In Part 2, EEG data collected in the above experiment was used to train an artificial neural network (ANN) to map EEG signals to machine commands. We found that our open-source ANN using spectrograms generated from SFFTs is fundamentally different and in some ways superior to Emotiv's proprietary method. Our use of novel combinations of existing technologies along with abstract and embodied imagery facilitates adaptive customization of EEG-BCI control to meet needs of individual users.

## DEDICATION

To my best friend and wife, Kirsten E. Cowan

## ACKNOWLEDGMENTS

I want to thank the following members of my graduate committee for their instruction and guidance throughout my graduate training: Clark Presson for inviting me to join the psychology program and for having faith in me despite my own doubts; Stephen Helms Tillery for introducing me to surgery, neural implants and brain-computer interfaces; Tom Sugar for his encouragement and introducing me to prosthetics; and especially Michael McBeath for guiding me through the layers of bureaucracy that seem to stop me in my tracks, and for teaching me statistics, as well as patience and perseverance. I also want to thank all the colleagues I have worked with in joint research projects during my long graduate tenure: Nick Thomas, Steve Holloway, Kristopher Jake Patten, Nancy Wechsler, and others too numerous to list here. Most of all I want to thank my now deceased parents who taught me to always question, observe, learn and create. They would have been proud of this moment.

## TABLE OF CONTENTS

	Page
LIST OF TABLES.....	vii
LIST OF FIGURES .....	viii
LIST OF SYMBOLS / NOMENCLATURE.....	x
PREFACE.....	xi
SECTION 1: THE TRANSFER OF MOTOR LEARNING	
CHAPTER	
1 INTRODUCTION.....	1
2 MOTOR LEARNING TRANSFER (MLT).....	4
3 EMOTIV® EEG-BRAIN-COMPUTER INTERFACE (BCI).....	9
4 DATA AQUISITION .....	13
EEG Calibration and Machine Control .....	15
5 EXPLORING MOTOR LEARNING TRANSFER .....	17
Hypotheses .....	17
Experimental Design.....	19
The Task and Associated Performance Measures.....	20
Participants.....	22
EEG-BCI Training.....	23
6 RESULTS .....	27
Proportion of ParticipantsAable to Learn EEG-BCI Control.....	27
Time Required to learn EEG-BCI.....	29

CHAPTER .....	Page
Learning Over Time.....	31
Motor Learning Transfer.....	35
7 DISCUSSION .....	43
Motor Learning Transfer.....	43
Abstract Imagery May be Better for EEG-BCI Control.....	44
SECTION 2: ARTIFICIAL NEURAL NETWORK FOR EEG SIGNAL PROCESSING	
CHAPTER	
8 INTRODUCTION.....	46
Artificial Neural Network Basics.....	46
EEG-BCI Artificial Neural Network Inputs .....	51
Network Architecture.....	60
Artificial Neural Network Performance .....	65
Network Performance With Data Averaging.....	70
9 SUMMARY AND CONCLUSIONS .....	73
Transfer of Motor Learning .....	73
Artificial Neural Network for Processing EEG Data .....	75
Take Home Messages .....	76
REFERENCES .....	78
APPENDIX	
A EXACT BINOMIAL DISTRIBUTIONS.....	84
BIOGRAPHICAL SKETCH.....	88

## LIST OF TABLES

Table		Page
1.	Experimental design .....	19
2.	Comparison of before and after means .....	39
3.	Processing ability as a function of hidden layers .....	61
4.	Parameter selection .....	64



## LIST OF FIGURES

Figure		Page
1.	The relative locations of electrodes .....	10
2.	Raw EEG signals during relaxation .....	11
3.	Raw EEG/EMG signals during physical movements .....	12
4.	The EPOC <sup>®</sup> headset .....	14
5.	The user interface for the pre- and post-practice test sessions .....	21
6.	EEG-BCI testing phase .....	25
7.	The interface for calibration and training .....	26
8.	The proportion of participants able to reach 50% correct.....	28
9.	The time required to learn EEG-BCI to criteria.....	30
10.	Evidence for learning BCI task to criteria.....	33
11.	The number of participants able to learn EEG BIC control.....	34
12.	Evidence for motor learning transsfer 1 .....	38
13.	Evidence for motor learning transsfer 2.....	42
14.	Basic ANN architecture .....	49
15.	The tanh(x) sigmoid function .....	50
16.	Power spectrogram of electrode P7 .....	53
17.	Power spectrum viewed through radial basis function.....	54
18.	Graphical depiction of SFFT .....	56
19.	Power spectrogram of “down” command .....	58
20.	Power spectrogram of “up” command .....	58

Figure		Page
21.	Power spectrogram of “neutral” command .....	59
22.	ANN performace in generating commands .....	67
23.	Averaging training samples.....	68
24.	ANN performace in generating commands with averaged samples.....	69
A1.	Probabilities with a fair coin .....	85
A2.	Cumulative probabilities with a fair coin.....	86
A3.	Cumulative probabilities with an unfair coin .....	87

## LIST OF SYMBOLS / NOMENCLATURE

### Symbol

1. AMI = Abstract Motor Imagery
2. ANN = Artificial Neural Network
3. BCI = Brain-Computer Interface
4. EEG = Electroencephalograph
5. EMI = Embodied Motor Imagery
6. EPOC<sup>®</sup> is a registered trademark of Emotiv corporation
7. MI = Motor Imagery
8. MLT = Motor Learning Transfer

## **PREFACE**

This document is divided into two sections. The first uses an electroencephalographic (EEG) brain-computer interface (BCI) to explore the phenomenon of motor learning transfer. The second takes a closer look at the EEG brain-computer interface itself and tests an alternate way of mapping EEG signals into machine commands.

Our primary goal is to better understand the roots of motor learning transfer (MLT). To that end we test whether MLT is more related to the use of shared neural structure between imagery and motor execution or to more generalized cognitive factors including attention, motivation and arousal. Experimental design and analysis of results are discussed in Chapters 1 through 7.

Our secondary goal is to explore alternate ways of mapping EEG signals into machine commands. To explore this we use an artificial neural network (ANN) to map EEG data into machine commands. This is further discussed in Chapter Eight.

## SECTION 1: THE TRANSFER OF MOTOR LEARNING

### CHAPTER ONE

#### INTRODUCTION.

Thorndike et al., (1901) first described the transfer of learning as the improvement of one mental function based upon the efficiency of another mental function. Since then, the transfer of learning has been studied in many contexts, from simple reaching movements to coordination dynamics and complex abstract thinking (Adams, 1987).

We are primarily interested in the transfer of *motor* learning skills, where speed and accuracy learned in one scenario facilitate learning a similar motor skill in another context. Ample experimental evidence suggests that practice using only motor imagery (MI) facilitates performance of the homologous physical task. Some have hypothesized that learning transfer results from the use of shared neural circuitry between imagined and physical tasks: practice with one leads to improvement in the other (Decety, 1996; Yaguez et al., 1998).

Though an appealing hypothesis, the fact that learning also transfers to non-homologous motor systems has led others to suggest that improvements in motor performance after motor imagery is a much more general phenomenon related to motivation, attention, general arousal and other cognitive processes (Paivio, 1985; Hall et al., 1998; Ste-Marie & Cumming, 2001). In a star line-drawing task, transference of skills occurred between distal and proximal musculature (Vangheluwe et al., 2004). Intermanual transfer of a complex finger tapping sequences transfers actually better from imagery than from actual physical practice (Amemiya et al., 2010). In all the aforementioned cases, improvements in performance transferred to non-homologous musculature, suggesting that

the cognitive components of the task may be more important than the motor components for learning transfer.

To test which hypothesis best models reality, we teach participants to control a machine using a brain-computer interface (BCI) and different types of mental imagery. Practice controlling a BCI using abstract disembodied imagery should only lead to improvements in performing the physical task if transfer is a general process involving motivation, focus, general arousal and other cognitive processes. If, however, transfer of motor learning is more related to the use of neural structures shared between imagined and physical tasks, then no learning transfer should occur after practice using disembodied abstract imagery for BCI control.

We chose an off-the-shelf EEG device from Emotiv, Inc. because it is non-invasive and relatively easy to use. The intricacies of this device and how it was used are discussed in Chapters 4 and 5. An EEG-BCI allows us to perform a physical task without engaging the neural structures normally associated with the motor execution of that task. We compare and contrast motor learning transfer (MLT) using embodied mental imagery (EMI) and disembodied abstract imagery (AMI). A control group merely practices physically performing a task for the same amount of time that the other groups mentally rehearse their assigned imagery tasks.

In EMI, the execution of the physical task is merely imagined thereby recruiting the use of neural structures normally associated with the performance of the actual physical task. In contrast, because abstract disembodied concepts are used in AMI, we engage neural structures that are not normally associated with the performance of a physical task. By comparing the transfer of motor learning in these three conditions (EMI, AMI, and control)

we provide evidence that supports either the notion that MLT results from the use of shared neural structures between imagined and physical tasks, or that it is a result of other mechanisms including motivation, attention and general arousal. If MLT results from the use of shared neural structures involved both in motor imagery and in the performance of the physical task, we would expect greater learning transfer when embodied motor imagery is practiced than when non-embodied abstract motor imagery is used. On the other hand, if MLT is more related to attention, motivation and arousal, then we would expect little difference in transfer between the EMI and AMI conditions.

Our secondary goal was to explore an alternate way of mapping EEG signals into machine commands. An off-the-shelf EEG-BCI was used to perform the above experiment. However, the process of mapping EEG signals to machine commands is proprietary. In chapter 8, we describe an alternate method of mapping EEG signals to machine commands using an artificial neural network (ANN) and short time interval FFTs. We suggest that this open source method of mapping EEG signals to machine commands will foster the development and proliferation of EEG-BCI technology for all and facilitate superior EEG control performance for a large variety of individuals.

## CHAPTER TWO

### MOTOR LEARNING TRANSFER (MLT).

There is already much experimental and clinical evidence to suggest that motor performance can be improved by mental imagery of the motor function in question. Perry (1939) used five tasks of different complexity (three hole tapping, card sorting, inserting round and square pegs into holes arranged in a grid, a more cognitive task where digits are substituted for symbols, and finally mirror tracing task). Imaginary practice improved performance in the actual motor execution of the five tasks to varying degrees. He found that five imaginary trials (300 seconds of total practice) in each task were as good as 4 actual peg board trials, 3 actual digit substitutions, 2 actual mirror tracings, 1 actual card sorting, and 1 actual hole tapping trials. Yaguez et al. (1998) used two tasks. He had subjects use ballistic movements to connect circles and draw identical figures at various scales. He found significant improvements in both speed and accuracy of movements after 10 minutes of imaginary practice doing the tasks. Gentili et al. (2010) found significant improvements in speed and accuracy in an arm pointing task after imagery practice. They also found partial improvement the task performance using the opposite arm in a mirrored task. Performance improvements suggested that subjects were able to internally simulate the dynamics and kinematics of their arm movements with apparently high precision. Debarnot et al. (2011) used mental imagery of finger tapping patterns rehearsed at different speeds and found that systematic increases in the speed of mental rehearsal did not translate to increased speeds in actual performance. However, mental rehearsal at any speed improved actual performance.



Perhaps more surprisingly, mental imagery seems to improve not only coordination, but also increases the amount of force muscles involved can generate. For example, in a four week training period, EMI increased strength in an isometric movement by 22% (as compared to 30% for actual movement) without increasing electromyographic (EMG) activity (Yue and Cole, 1992; see also Ranganathan et al., 2004). Reiser et al., 2011 combined different proportions of imaginary muscular contractions with actual isometric contractions. They concluded that significant strength gains can be achieved even when up to 75% of physical training units are replaced by imaginary units.

As a result, mental imagery is being increasingly used in strength training and rehabilitation (Silvoni et al., 2011 - stroke rehabilitation; Reiser et al., 2011 - strength training; Page et al., 2011 - stroke rehabilitation; Silvoni et al., 2009 - Amyotrophic Lateral Sclerosis (ALS); Buttler and Page, 2006 - stroke rehabilitation).

Why should the aforementioned improvements in physical performance occur as a result of mental imagery? Neurophysiological studies have reported that imagined movements and physically executed movements involve the same neural substrates (Miller et al. 2010; Ehrsson et al., 2003; Jeannerod 2001; Filimon, 2004). Because imagined movements share the same temporal and kinematic relationships, neural infrastructure, and autonomic responses (heart and respiration rates) as the corresponding physical movements, it is reasonable to expect that practice in one will have some impact on the other (Decety, 1996; Yaguez et al., 1998).

Although appealing, the above theory does not account for the fact that transfer of motor learning also occurs when one practices a motor task with one set of muscles and later tests performance with another. For instance, right-hand learning of a finger maze

enhanced opposite hand performance learning in a vertically flipped maze, while left-hand learning enhanced opposite hand learning on a mirror reversed maze regardless of hand dominance (Stoddard and Vaid, 1996). In a star line-drawing task, transfer of skills occurred both from gross motor movements to fine motor movements, as well as, from fine motor to gross motor (Vangheluwe et al., 2004). In fact, Yasuda and Miyamura (1983) found that even unused ipsilateral musculature strength is improved after embodied motor imagery (EMI). Amemiya et al. (2010) suggested that if motor execution and corresponding feedback is important for intermanual transfer, then motor execution would lead to more intermanual transfer than imagery. However, if abstract knowledge acquired during training is more important, then intermanual transfer during imagery would be equal or greater for imagery than motor execution. Using a complex finger sequence tapping task, they found that intermanual transfer was greater for imagery than for the manual execution groups. Keeping in mind that EMI activates somatotopically organized sections of the primary motor cortex in a systematic manner and activates body-part-specific representations in the nonprimary motor areas (Ehrsson et al., 2003), learning transfer to non-homologous areas suggests that motor transfer involves more than the activation of homologous neural structures. If networks for activating different body parts are different, how then can motor learning spill out into areas not directly involved in the imagery task? The above findings suggest that the transfer of motor learning must be a far more general process than the shared neural structures hypothesis presumes. Transfer of motor learning to different body parts involving different neural structures suggests that the transfer of motor learning has more to do with arousal, attention, mental exercise or other cognitive process (Paivio 1985; Hall et al., 1998; Ste-Marie and Cumming, 2001). So far, the transfer

of motor learning has been investigated in neural mechanisms involved in an embodied framework<sup>1</sup>. That is, when one imagines moving one's limbs as if one were physically performing a task, one becomes better at physically executing the task. Using an EEG device with mental imagery is essentially the same thing except that a physical task is executed by a machine as a direct result of imagery. When one practices imagining a motor act to elicit a response from a properly calibrated EEG-BCI, the embodied mental imagery (EMI) should translate to measureable improvements on performance of the actual physical task.

To test whether rehearsal with mental imagery transfers to physical performance because of activation of homologous neural structures or because of more general cognitive processes we trained participants to use an EEG-BCI device to control a mouse on a computer screen using two distinct types of imagery. First, participants imagine moving their arms and fingers to move the cursor while keeping their arms and fingers resting comfortably on their laps. We then use the corresponding EEG patterns to generate control signals to move the mouse on the screen. If only rehearsal with EMI leads to improvements in the physical performance of the task, this will support the notion that it is the exercise of neural resources used in common between imagery and physical practice that leads to transfer. In contrast, if transfer also occurs when participants imagine disembodied abstract concepts, thereby engaging neural structures not involved in performance of the physical task, this will support the notion that transfer is the result of more general cognitive processes including attention, motivation, and arousal.

---

<sup>1</sup> Embodied also includes a third person perspective (as in seeing oneself perform an action).

We explore if practice visualizing abstract concepts (AMI), as opposed to visualizing embodied tasks (EMI) also translates to improvements in the actual performance of physical tasks. Using abstract thought to control a device is an important consideration<sup>2</sup> since the target of some BCI systems are those with motoric handicaps due to some disruption in their neural infrastructure. Controlling tasks by contemplating abstract ideas may be particularly relevant for people with Amyotrophic Lateral Sclerosis (ALS)<sup>3</sup> whose primary motor cortex activation is reduced or altered (Stanton, et al., 2007; Riva et al., 2012), and people with Parkinson’s disease<sup>4</sup> or for stroke survivors who may be suffering from reduced motor abilities. Patients with left frontal and right posterior parietal lesions, for instance, are unable to imagine a motor task (Johnson, 2000). Contemplating abstract thoughts instead of visualizing embodied movements may offer an alternative means of machine control for these individuals. Contemplating abstract thoughts as a means of machine control may also produce EEG signals less contaminated by concurrent observations of the movement of others. These “cleaner” signals may be a benefit for EEG-BCI control in general. A comparison of EEG-BCI control using EMI or AMI will be done in Chapter 7

---

<sup>2</sup> Kostov and Polak , 2000 were the first to mention the possibility of using abstract thoughts to produce EEG signals for use in BCIs, but to our knowledge it has not been well tested.

<sup>3</sup> ALS is a degenerative disease that affects the metabolism of motor neurons in the cortex and spinal cord. Because the primary motor cortex is involved in motor imagery (Snitzler et al., 1997), it is likely that motor imagery in ALS patients will also be adversely affected.

<sup>4</sup> Yaguez et al., 1999 showed those with Parkinson’s disease did *not* benefit from motor imagery, whereas person’s with Huntington’s disease did.

## CHAPTER THREE

### **EPOC<sup>®</sup> EEG BRAIN-COMPUTER INTERFACE (BCI).**

In a typical EEG-BCI, participants generate a control signal by imagining the movement of their arms or fingers (embodied homologous mental imagery). To move a cursor up or down, a person simply imagines moving the cursor up or down with his or her arm or finger. The unique constellation of EEG patterns generated with each period of mental imagery are then mapped to desired commands, which can be used for controlling a device.

However, theoretically, any consistently distinguishable signal can be used for control. We therefore also asked some participants to contemplate abstract disembodied concepts (e.g. happiness, fulfillment, regret, justice). Then, just as with embodied imagery, we mapped the corresponding EEG signatures to specific control signals (up, down, or neutral).

EEG signals are a time series of voltages read at the surface of the scalp. The locations of the electrodes and their associated names are depicted in Figure 1. EEG signals are notoriously noisy and impossible to interpret without the aid of sophisticated mathematical analysis. Figure 2 shows a typical time sequence of raw EEG data. It is important to note that the skull acts as a low pass filter (i.e. permits only low frequencies to pass). Signals reaching the surface are relatively weak compared to electromyographic (EMG) signals emanating from the musculature on the surface of the skull. Figure 3 a-d shows how EMG signals completely overshadow EEG signals when cranial musculature is activated. These figures are presented for three reasons. First, they demonstrate that EMG signals are easily distinguishable from EEG signals by their amplitude. Weak EMG

signals are, however, an unremovable confound. Secondly, these figures highlight the importance of remaining relaxed and as immobile as possible during EEG recordings and EEG-BCI control. Finally, these figures suggest that the amplitude of the signals may be used as a marker for EEG vs. EMG signals. A more detailed discussion on how to interpret these raw EEG signals follows in Chapter 4.

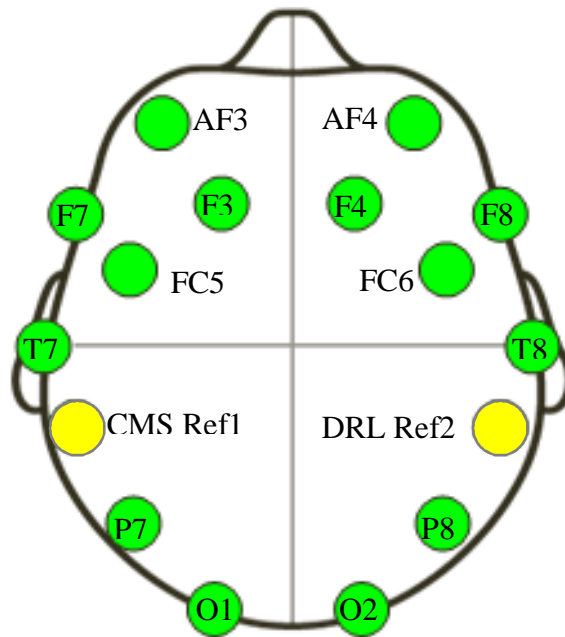


*Figure 1.* The relative locations of electrodes used in this document and their associated labels.

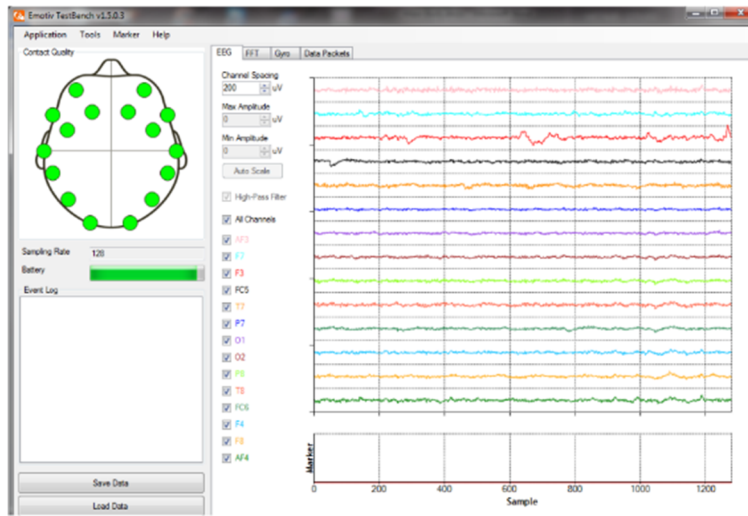


*Figure 2.* Raw EEG signals from the 14 electrodes depicted on the surface of the skull at the top left of the figure. The signals are from a user sitting still in front of a monitor in a relaxed state.

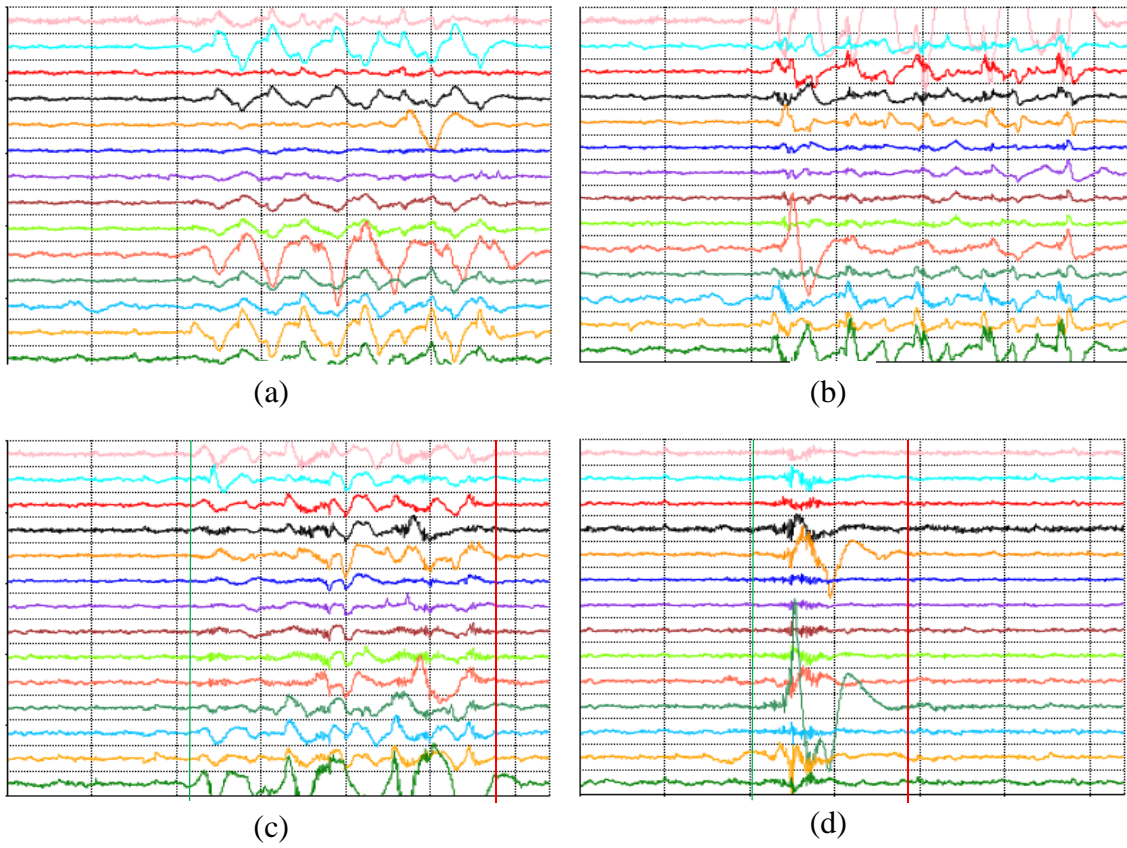


*Figure 3.* EEG/EMG data. Low amplitude waves correspond to EEG signals. (a) High amplitude waves correspond to the subject's eyes moving side to side. (b) High amplitude signals correspond to the eyes moving up and down. (c) Moving the head up and down. (d) Swallowing. The green and red vertical lines indicate the onset and end of muscle activity.



## CHAPTER FOUR

### DATA ACQUISITION.

Figure 4 shows the wireless EPOC<sup>®</sup> headset used for collecting EEG signals. We chose an EPOC<sup>®</sup> EEG headset for several reasons. First, it is compact and wireless. Second, it is relatively inexpensive and easy to use. Thirdly, a software development pack is available that allows us to write custom code for any application we wish to develop. Finally, we were able to retrieve and record all 14 channels of EEG data in “real” time.

Machine commands along with the EEG readings associated with those commands are transmitted wirelessly every 100ms or so. Although each electrode is sampled every 7.8 ms, they are unfortunately not time stamped. It is therefore necessary for the computer receiving the EEG signals to back timestamp the signals relative to the time the packet of signals was received.

The electrodes are made of a felt material which must be kept moist with a saline solution (i.e. contact lens solution) in order to maintain electrical conductivity. Though simple to use, the fact that electrodes must be kept moist makes the machine unsuitable for long term continuous use. It is, nonetheless, useful as a research tool.



*Figure 4.* The wireless EPOC® headset. There are 14 useable electrodes in all: 8 frontal electrodes, 2 reference electrodes, 2 occipital, 2 temporal, and 2 parietal electrodes. Two accelerometers are also available to detect movement forward and back as well as side to side. We elected not to use these signals at this time.

## **EEG CALIBRATION AND MACHINE CONTROL**

The EPOC<sup>®</sup> wireless headset must first be calibrated for each participant. To calibrate, users must hold an image in mind for 8 seconds while the apparatus records the EEG traces of 14 electrodes placed on the scalp. The set of EEG traces recorded for that 8 second interval are then assigned to a particular control command (i.e. move cursor up, down, or keep still). After each 8 second calibration, the participant reimagines what they previously held in mind for 8 seconds in an attempt to move the cursor. This process is repeated several times until the user can reliably move the cursor in the desired direction by reproducing the EEG pattern recorded for each control signal. Participants may require many recordings before the apparatus can reliably distinguish consistent differences in the EEG traces. Indeed, many participants were unable to produce reliably repeatable signals necessary for machine control in the two hour period allotted for the experiment described in Chapters 5-7. I himself required several hours over a one week period before reliable control could be achieved. We presumed that the ability to stay focused and consistently reproduce the imagery used when recording without extraneous signals is paramount. The algorithm used for this decoding is proprietary to Emotiv Corporation. We attempted our own method of decoding EEG signals in Chapter 8.

The EEG-BCI basically consists of the EEG apparatus and C++ and Python code to map EEG signals and EPOC<sup>®</sup> commands into actions on a computer. The C++ program simply collects the EEG signals and EPOC<sup>®</sup> commands, then sends the resulting data packets to the receiving application. Each data packet consists of an EPOC<sup>®</sup> derived machine command and the preceding EEG signals leading up to that command. The Python program receives the EEG data and EPOC<sup>®</sup> commands and converts them into

mouse movements on the screen. Here we focused on just three commands: moving the mouse up, down, and remaining motionless (neutral).

The code for both of these programs is freely available by contacting the author at [flavio.dasilva@asu.edu](mailto:flavio.dasilva@asu.edu). As mentioned earlier, calibration and training is an iterative process. Calibration involves recording 8 sec EEG samples of the user relaxing and clearing their mind, imagining moving their arm and fingers up and down, or imagining distinct disembodied abstract concepts. The recorded EEG patterns are then assigned to one of three controls: up, down, or neutral. Once calibrated, it becomes the user's job during training and practice to learn to recreate, as close as possible, the EEG patterns generated during calibration. Several EEG recordings are made of each desired control command using assigned imagery method, interspersed with periods of practice until the user achieves a certain level of competence and confidence. Miller et al. (2010) have shown that with feedback, participants can learn to modify both their high (76-100 Hz) and low frequency (8-32 Hz) cortical surface potentials. Although Miller et al. (2010) used electrocorticography (ECoG)<sup>5</sup> instead of EEG, Miller's low frequency range (8-32 Hz) is compatible with non-invasive scalp surface EEG recordings. Therefore, we were confident that users would be able to learn adequate machine control using EEG. A more precise description of the training process is discussed in Chapter 5.

---

<sup>5</sup> ECoG is a method of recording electrical activity in the brain by placing electrodes directly on the surface of the brain, bypassing the skull)

## CHAPTER FIVE

### EXPLORING MOTOR LEARNING TRANSFER

#### **Hypotheses.**

We have several distinct hypotheses about motor learning transfer from mental imagery practice and performance using an EEG-BCI. First, because abstract imagery is more distributed throughout the brain than the imagined motion of one's arm and finger, we expect that it will be easier to learn EEG-BCI using abstract imagery than embodied imagery. That is, we expect more participants to be able to master EEG-BCI when using abstract imagery than when using embodied imagery ( $H_{1a}$ ). We also expect that the time required to master EEG-BCI will be less for those using abstract imagery than those using embodied imagery ( $H_{1b}$ ):

$$H_{1a}: N_{abstract\ BCI} > N_{Embodied\ BCI} \quad (1)$$

$$H_{1b}: T_{abstract\ BCI} < T_{Embodied\ BCI} \quad (2)$$

Secondly, we expect that if motor learning transfer occurs at all, the mean  $RMS_{error}$ <sup>6</sup> in performing the actual motor execution of the task will be smaller after practice than before practice for all three conditions:

$$H_{2a}: RMS_{Error\ before} > RMS_{Error\ after} \quad (3)$$

If motor learning transfer (MLT) is due to the shared use of neural structures between imagery and motor execution, then the mean MLT should be greater for the embodied group than for the abstract group. That is, the reduction in RMS error should be

---

<sup>6</sup> See page 20

greater for the embodied group than for the abstract group ( $H_{2b}$ ). Furthermore, we expect that the number of participants who showed MLT will be greater in the embodied group than in the abstract group ( $H_{2c}$ ).

$$H_{2b}: \Delta RMS_{Error\ embodied} > \Delta RMS_{Error\ abstract} \quad (4)$$

$$H_{2c}: N_{EmbodiedMLT} > N_{Abstract\ MLT} \quad (5)$$

On the other hand, if motor learning transfer is due to motivation, arousal, and other psychological factors, and assuming both groups are equally motivated, the mean MLT (or the reduction in RMS error) should be the same for the embodied and abstract groups ( $H_{2d}$ ). In addition the number of participants who demonstrate MLT would be the same for both groups ( $H_{2e}$ )

$$H_{2d}: \Delta RMS_{Error\ embodied} = \Delta RMS_{Error\ abstract} \quad (6)$$

$$H_{2e}: N_{EmbodiedMLT} = N_{Abstract\ MLT} \quad (7)$$

We expect that manual motor practice will, of course, produce the most learning transfer from practice to execution.

$$H_3: \Delta RMS_{Manual} > \text{or}(\Delta RMS_{Error\ embodied}, \Delta RMS_{Error\ abstract}) \quad (8)$$

### Experimental Design.

We chose a 2x3 within subjects design to compare each participant's ability to perform a physical task pre- and post-training (see Table 1). We divided 36 subjects into three groups. Group 1 learned to control the cursor by imagining moving their arm and finger and used the associated EEG signals to control the cursor. Group 2 learned to control the cursor by contemplating different abstract (disembodied) concepts (e.g. courage, fear, justice, freedom, etc.) and used the associated EEG signals to control the cursor. Group 3, the control group, merely practiced moving the cursor by physically touching the computer screen and moving their arm and finger up and down. The same pre- and post-training manual performance measures were taken for each member of each group. Each group received as much training as required (up to 1.5 hours) to learn to control the cursor using one of the two methods of EEG control (embodied and abstract imaging).

Table 1. *Experimental design is a 2 x 3 within subjects design.* Each participant's ability to manually perform the motor task will be measured before and after one hour of training in one of three conditions: abstract imagery, embodied imagery, and actual physical practice.

Type of practice 1 – 1.5 hours)			
	Embodied Imagery	Abstract Imagery	Physical (Control)
Pre-practice	Performance measure	Performance measure	Performance measure
Post-practice	Performance measure	Performance measure	Performance measure

### **The Task and Associated Performance Measures.**

In order to measure learning transfer, we used a sine wave tracking task similar to Carey (1990) and Carey et al. (2002). Participants are required to move a cursor up or down in order to follow a target bobbing up and down on an oscillating sine wave moving horizontally across a computer touch screen. A touch screen was used (Dell Inspiron 1090) so participants could freely slide their index finger up and down on the screen to move the cursor. A trial consisted of moving the cursor (with a finger on a touch screen) so that it remained as close as possible to the target moving up and down for one minute. Figure 5 shows a fictitious participant performing the physical task.

The root mean squared error between the vertical position of the cursor and the target was used to assess the participant's ability to physically perform the motor task. The root mean squared error was computed as follows:

$$RMS_{error} = \sqrt{\frac{\sum(Cy - Ty)^2}{N}} \quad (9)$$

Where:

Ty = the vertical position of the target (red ball)

Cy = the position of the cursor (white ball) controlled by the participant

N = is the number of samples (recorded at 100 times per second)

Learning transfer was assessed by comparing each participant's cursor tracking ability, the  $RMS_{error}$ , before and after an hour of training using one of three methods to move the cursor: 1) Embodied Motor Imagery: using EEG signals generated by only imagining moving one's finger and arm up and down on the screen, 2) Abstract Motor



Imagery: using EEG signals obtained by contemplating more abstract concepts like love, hate, and justice to move the cursor, or 3) Physical Movement: using only index finger and arm movements on a touch screen as in the pre and post training trials. Five one minute pre- and post-BCI EEG training test trials were used to assess the participant's ability to perform the tracking task.

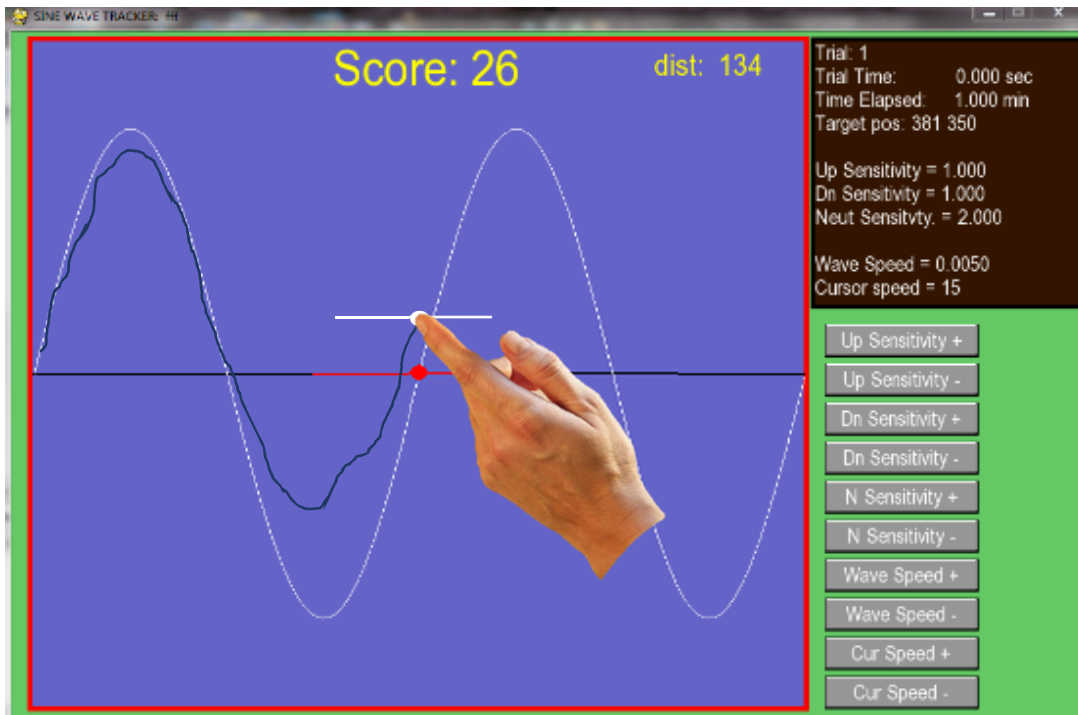


*Figure 5.* The user interface for the pre- and post-practice test sessions. This shows a sample of the display presented to the user along with a blue trail generated by their cursor movements. The white line is an oscillating sine wave moving to the left. The computer tracks the vertical direction of the sine wave as it passes through the center of the screen with the red ball and line. In this figure, the participant manually moves the white ball by touching the screen with his/her finger and moving it up and down. This manual method of moving the cursor was used to assess the participant's ability to track the moving red cursor before and after training. During training only, each participant was assigned to practice moving the white cursor up and down using one of the three methods described above (see text). The dark blue line shows the history of the participant's movements.

## **Participants.**

Participants were recruited from the pool of graduate and undergraduate research assistants in the psychology and bioengineering departments as well as many volunteers from an undergraduate statistics class who earned extra credit for their participation. All participants signed informed consent forms and the experimental protocol was carried out in agreement with legal requirements and international norms in accordance with the Institutional Review Board (IRB). Participants were not detained more than two hours, and were informed to take as many breaks as necessary to prevent fatigue. All participants indicated that they chose to volunteer because they were interested in learning to control a machine using only their thoughts. As a courtesy to those who were randomly assigned to the control condition (to physically practice moving the cursor up and down using their finger for an hour), we allotted forty-five minutes at the end their session to teach them how to use EEG for machine control.

Following recommended Emotive protocol, participants were situated in a quiet room and fitted with the EPOC<sup>®</sup> EEG apparatus (Figure 4) which was adjusted and moistened with saline solution until all electrodes provided a consistently strong signal. EEG signals were acquired while participants sat upright in a chair with hands resting in their laps at arm's length away from a computer monitor. Participants were then instructed to relax their muscles and remain still to reduce undesirable noise in the EEG signals. Participants with particularly thick hair, wearing hair extensions, or with any other characteristic that made EEG signal reception impossible were discontinued from the trials. Only one participant during pilot testing had to be rejected for these reasons.

### **EEG-BCI-Training.**

Prior to use, the EPOC<sup>®</sup> wireless headset must first be calibrated for each participant. After moistening each electrode, the apparatus was placed on the participant's scalp such that the front electrodes were three finger widths from the top of the brow, and the two reference pads are comfortably situated on the bone behind the ears (the mastoid process). Participants were then informed to sit relaxed in front of a computer monitor with their hands comfortably on their laps. Prior to calibration, participants were also shown a graphical representation of their EEG signals (Figure 2). They were then asked to cough, frown, smile, and move parts of their body as they observed the patterns of the EEG voltages (as in Figure 3). This was done so we could stress the importance of remaining still and calm throughout the experiment.

Once the above preliminaries were completed, participants were asked to clear their minds and relax with their eyes open while their EEG patterns were recorded for eight seconds. These EEG patterns were then assigned to the *neutral* command. Next, participants were again asked to relax and keep their eyes open as they imagined either moving the cursor up using their finger and arm, or to imagine a previously agreed-to abstract concept per their assigned condition. During this 8 second mental imagery period, we again recorded the EEG signals and assigned them to the *up* command. Finally, we asked the participants to remain relaxed for another eight seconds as they imagined either moving the cursor down with their finger and arm, or another distinctly different pre-agreed-to abstract concept. These EEG recordings were assigned to the *down* command. Once this preliminary calibration was completed, the cursor began to move and participants

were allowed to practice moving the cursor up and down by repeating their pre-recorded mental imagery.

Initially, performance may appear random, in which case more calibration recordings are done as described above. Periodic testing is performed to assess participants' level of control. Testing is performed as depicted in Figure 6. The fixation phase is coincident with an audible "beep" and remains visible for one second. An instruction then follows which remains visible for 3 seconds. The instruction and fixation cross is then removed as the to-be-controlled cursor appears for 10 seconds. During this phase, the participant attempts to move the cursor as instructed by using the same mental imagery used during the recording phase. The percentage of cursor moves that were consistent with the instruction are prominently displayed at the edge of the screen. In the embodied condition, the words "up", "down", or "neutral" will appear on the instruction screen. In the abstract condition, a single word will appear to remind participants of the pre-agreed-to abstract concept to be imagined. Depending on the result of the testing, more eight second recordings of each of the command conditions may be warranted. This iterative calibration and training process is continued until the participant is either able to correctly produce up, down, and neutral commands 50% of the time or their allotted time is up. Note that the correct move will be performed correctly 33% of the time by chance). If and when the participant is able to perform each of the desired moves 50% of the time, EEG calibration is fixed. The resulting calibration parameters remain unchanged throughout the remainder of the training period. Since the participant's intent is presumably consistent with the instructions given on the screen, these recordings are later used to train the neural network discussed in Chapter 8.

Once participants reached the minimum of 50% correct on each of the commands, they were then given the option of practicing using imagery to cause the cursor to follow the moving sine-wave target using the same screen that was used during the physical task (except with EEG-BCI control this time), or to continue practicing as in the calibration phase. In either case, mental imagery for control was practiced for one hour. During this practice phase participants were encouraged to take as many small breaks as needed to avoid fatigue.

After one hour of practice moving the cursor in the assigned condition, participants were given a few moments of rest. After this small resting phase (5 minutes or less), each participant was again tested on their ability to manually track the moving target by using their finger to move the cursor on a touch screen as they did prior to EEG-BCI training. The ability to control a cursor using the EEG-BCI, as well as the assessment of motor learning transfer, is discussed in the next chapter.

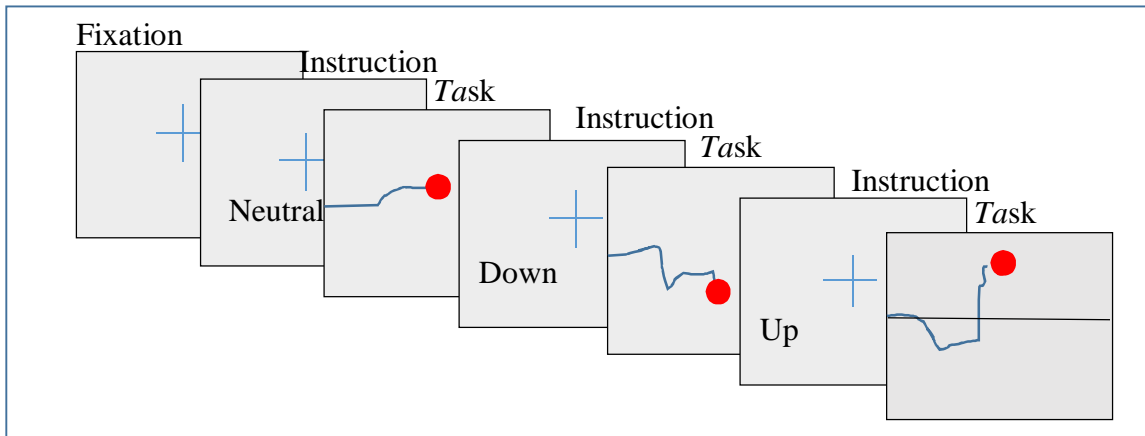


*Figure 6.* EEG BCI testing phase. The process starts with a 1 sec fixation screen, followed by a 3 sec instruction (“up”, “down” or “neutral” in the embodied condition, or the agreed upon abstract concept in the abstract condition). After the three second instructions, the participant is given 10 sec to move the cursor using only their thoughts. The process is repeated for each command.

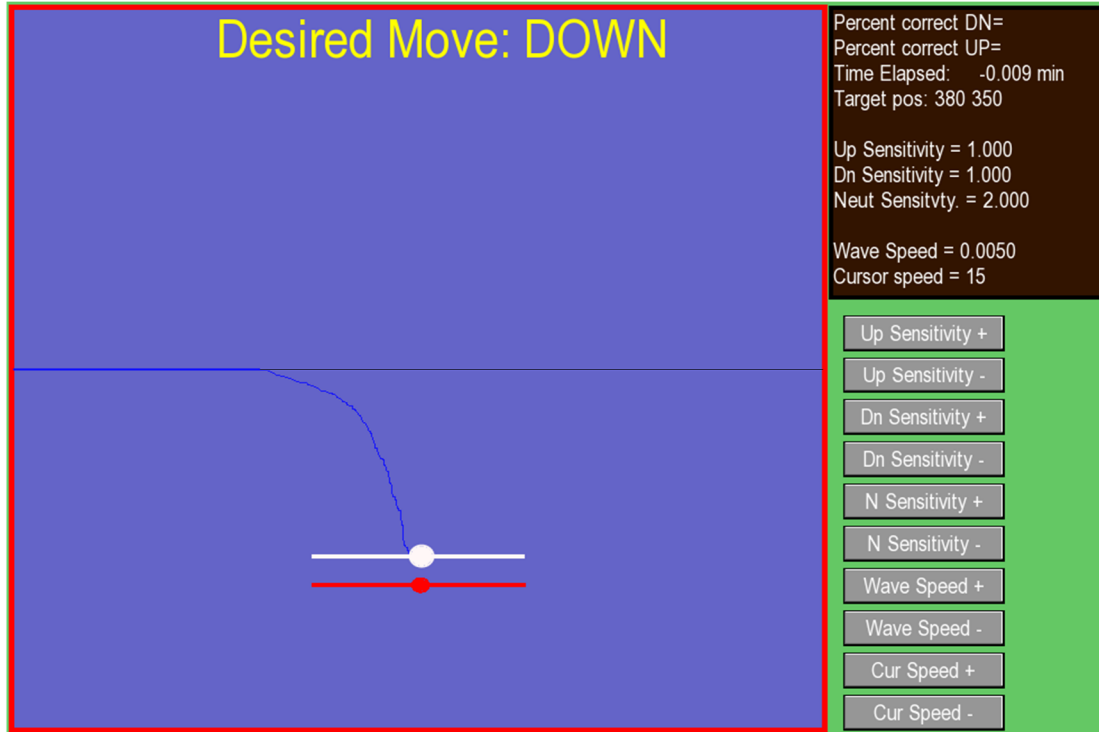


*Figure 7.* The interface for calibration and training. The user is instructed to imagine an abstract concept or an embodied motion for 8 seconds. The resultant EEG patterns are assigned to a particular cursor direction. After each 8 second session the cursor is allowed to move when the user again imagines as instructed. If the cursor moves in the appropriate direction as instructed 50% of the time, the machine is considered properly calibrated.

## CHAPTER SIX

### RESULTS

#### **Proportion of participants able to learn EEG brain-computer control.**

First, it is important to note that not all participants were able to learn to control the cursor with the EEG signals emanating through their skulls. Figure 8 (a) shows the proportion of participants that were able to learn to criteria (LTC). LTC indicates that a participant was able produce the desired machine command (up, down, or neutral) a minimum of 50% of the time as compared to random which is 33.33%. Because participants volunteered for the study in order to learn EEG machine control, we allotted 45 minutes after all training and testing was completed to teach the control group how to use EEG signals for machine control to prevent them from becoming disappointed. Figure 8 (b) shows the proportion of those in the control group, who practiced the physical task for an hour first, that were able to learn to criteria within the last 45 minutes<sup>7</sup>.

There were no statistically significant differences in the proportion of participants that were able to LTC using abstract imagery versus embodied imagery (two-tailed t-test, mean proportion change = 0.25,  $t(22)=2.074$ ,  $p=0.237$ ). Only 41% embodied versus 66% of abstract participants were able to learn EEG-BCI control to the 50% correct LTC level in the time allotted. There also was no statistically significant difference between those who practiced the physical motor task first and those who did not in terms of the proportion of participants able to learn control in the time allotted (two-tailed t-test,  $t(33)=1.193$ ,  $p=0.242$ ).

---

<sup>7</sup> Randomized between EMI and AMI

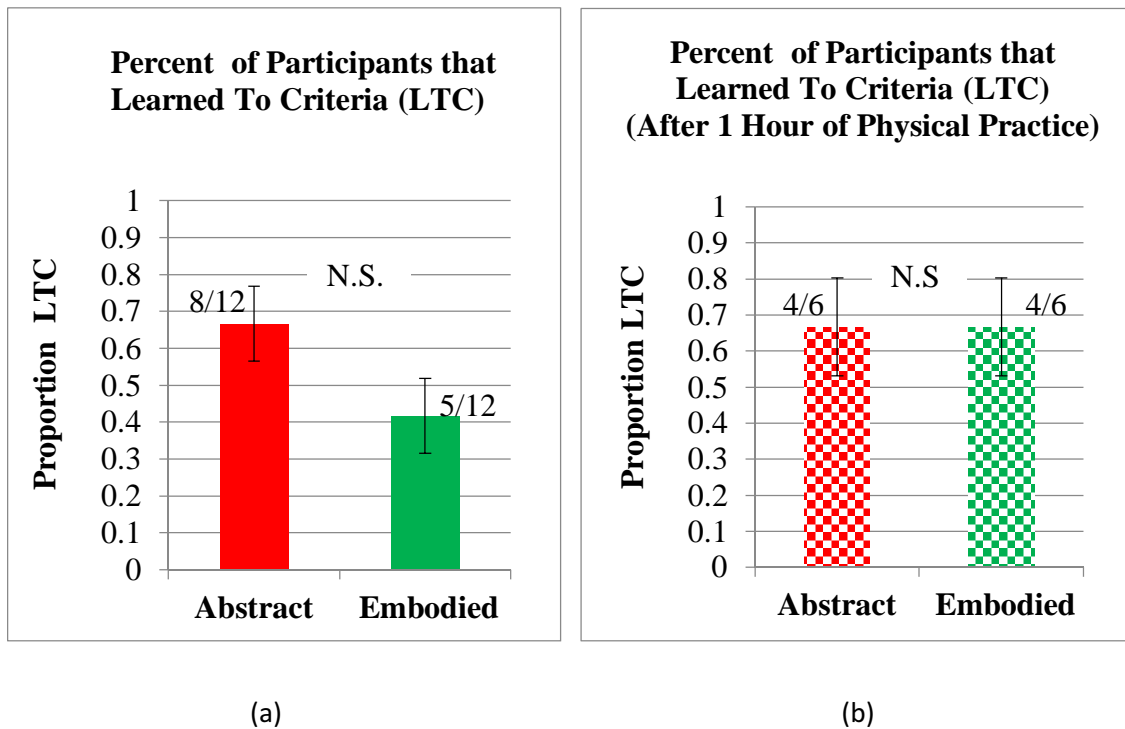


*Figure 8.* (a) The proportion of participants that were able to reach a minimum of 50% correct on each of the machine commands (up, down, and neutral). Error bars are std error (Stdev/Sqrt(N)). The differences between those using abstract imagery and embodied imagery were not, however, statistically significant (mean proportion change = 0.25, two-tailed t-test,  $t(22)=1.216$ ,  $p=0.237$ ). (b) The proportion of control participants that were able to learn each of the machine commands to criteria. The differences are not statistically significant (mean proportion change = 0.0, two-tailed t-test,  $t(6)=0$ ,  $p=1.0$ ). No significant differences between those who physically practiced using their finger for an hour first, then subsequently learning EEG BCI, from those who attempted to learn BCI without prior finger practice (mean proportion change = 0.18, two-tailed t-test,  $t(33)=1.193$ ,  $p=0.242$ ).



### **Time required to learn EEG-BCI.**

The time it took for each group to learn control to criteria (50% correct) is shown in Figure 9 (a and b). The first figure shows that on average, it took about seventeen minutes to learn EEG brain-computer control for those that were actually able to learn. There was no significant difference in the amount of time it took to learn the control task between the embodied and abstract groups (mean time difference = 2.68 min, two-tailed t-test,  $t(9) = -.298$ ,  $p=0.773$ ). Interestingly, however, there was a marginal learning advantage for members of the control group who practiced the physical task for one hour first to learn control using embodied imagery (mean time difference = 15.77 min, two-tailed t-test,  $t(5) = -2.215$ ,  $p=0.077$ ). This phenomenon may warrant further study at a later date.

The above findings are in direct contradiction to what was expected in Hypothesis 1<sub>b</sub>. That is, the number of participants able to learn EEG-BCI (as measured by our LTC) using abstract imagery was not greater than the number of participants who used embodied imagery. Additionally, the time to LTC, was not different for the two groups. However, in retrospect, using a one-time measure of LTC (i.e. 50% correct on up, down, and neutral moves) may not have been the best measure of learning. Another measure of learning will be discussed in the next section.

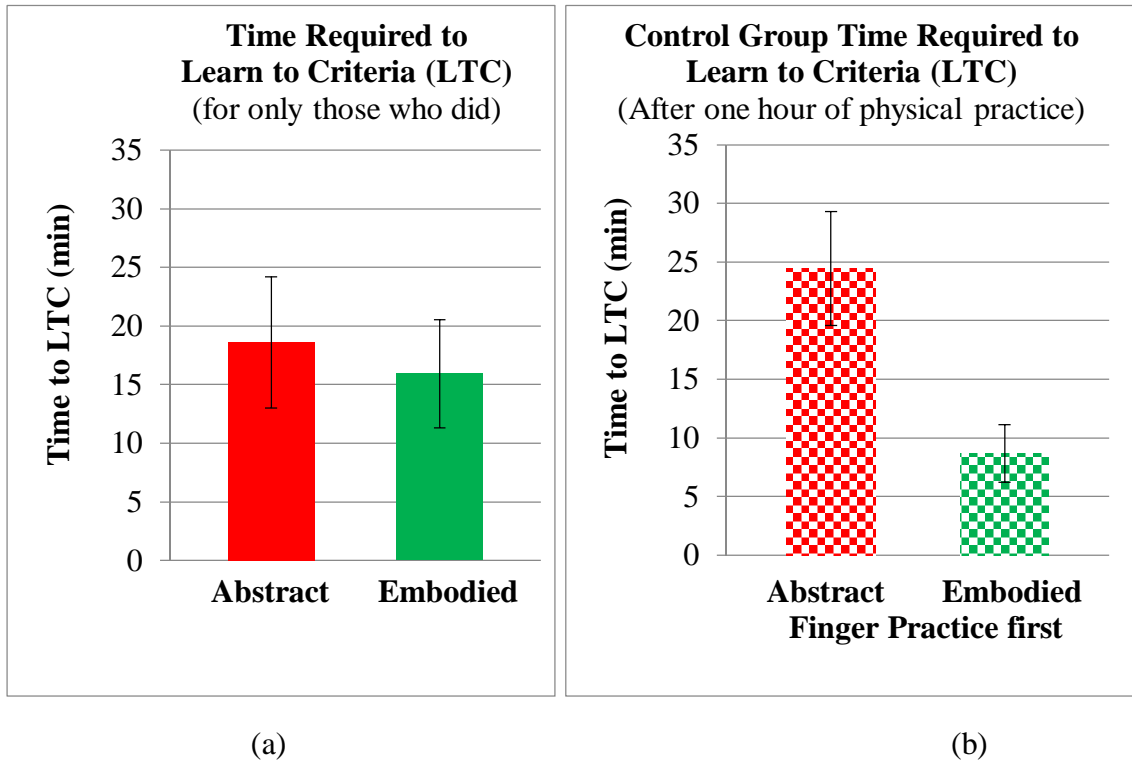


*Figure 9.* (a) The time required to learn EEG BCI to criteria (for those who were able to learn). Error bars are std. error (Stdev/Sqrt(N)). The differences are not, however, statistically significant (two-tailed t-test,  $t(9) = -.298$ ,  $p = 0.773$ ). (b) The amount of time required to learn EEG BCI to criteria after an hour of physical practice. The differences are not quite significant (two-tailed,  $t(5) = -2.215$ ,  $p = 0.077$ ). Low  $df$  values reflect adjustments for unequal variances.

### **Learning over time (continuous cycle RMS errors).**

Figure 10 shows the performance of a single subject over the course of practice. A performance test was taken approximately every two minutes. With practice, this participant not only improved their mean percent correct moves (up, down, or neutral), they also decreased the standard deviation of the percent of correct moves. The slopes of the percent correct and standard deviation curves were both significantly different from zero, indicating that EEG-BCI control performance improved over time (Regression of Mean % Correct,  $F(1,28) = 8.12, p=0.008$ , regression of the standard deviations of the percent correct moves,  $F(1,28) = 7.29, p=0.012$ ).

In retrospect, this regression of the mean percent correct is a better method of assessing competence in EEG-BCI control than the one-time reaching 50 % correct reported earlier. A participant could have reached a one-time 50% correct on up, down, and neutral moves by chance alone. Whereas a statistically valid test would have been more appropriate. When we use regression to distinguish those who were able to learn EEG-BCI from those who were not we found that 5 out of 12 participants (41.7%) who used abstract imagery marginally improved their BCI performance during the practice period (positive slopes with  $p<0.1$ ). In contrast, only 1 out of 12 participants (8.3 %) who used embodied imagery improved their BCI performance during the practice period.

The probability of getting exactly  $k$  or more participants out of 12 who improve their performance during practice is expressed in the cumulative binomial probability mass function (where  $N = 12$ , and  $p=0.5$ ):

$$P(x \geq k) = \sum_{x=k}^N \left( \frac{N!}{x!(N-x)!} p^x (1-p)^{(N-x)} \right) \quad (10)$$

For a sign test,  $p$  is set at 0.5. A sign test should indicate if the number of participants who merely improved their scores could have occurred by chance. If we are interested in the number of participants who significantly improved to  $p < 0.1$  or  $p < 0.05$  levels, then we set  $p = 0.1$  or  $0.05$  respectively. The number of participants who improved their percent correct scores during practice in each condition is shown in Figure 11. The probability of getting 5 or more participants who improved their scores to the  $p < 0.1$  level is significant ( $p = 0.0038$ ). However, the probability of having one or more participants improve to the  $p = 0.1$  level is not significant ( $p = 0.377$ ). Appendix A has a discussion on binomial distributions and shows the probabilities of the number of participants who should improve to different significance levels. It seems, therefore, that EEG-BCI control may be easier to learn using abstract imagery than embodied.

In contrast to Figures 8 and 9, Figure 11 provides direct confirmation of hypothesis  $H1_a$  described above. As we suspected, the number of participants able to learn EEG-BCI control in the allotted time was greater for those who practiced abstract imagery than for those who practiced embodied imagery. As indicated earlier, we suspected that this would be the case because embodied EEG signals are more or less confined to the premotor and motor cortices, whereas abstract concepts can be more widely distributed over the entire brain. As a result, we suspected that EEG signals for abstract concepts would be easier to distinguish than EEG signals for imaginary up and down moves.

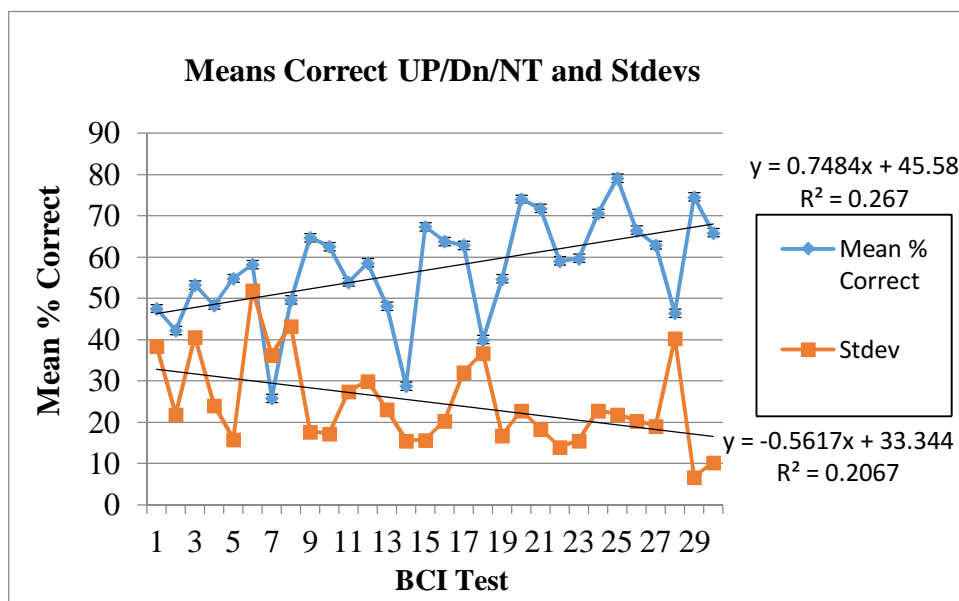


*Figure 10.* Evidence for learning BCI task. The mean percent correct and std. deviation for up, down, and neutral moves for a single participant as a function of time are shown above. This participant clearly shows learning over the course of one hour of practice. BCI test performed around every two minutes. With more practice, the Mean % correct increased significantly, (Regression of Mean % Correct,  $F(1,28)=8.125$ ,  $p=0.008$ ). The standard deviations of the Mean % correct correspondingly decreased with practice (Regression of Stdev,  $F(1,28)=7.29$ ,  $p=0.011$ ). Not all participants showed this pattern of improvement.

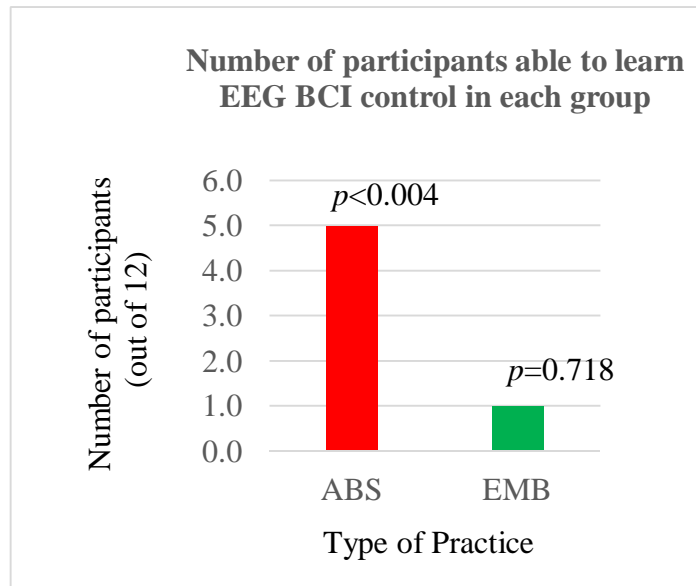


*Figure 11.* The number of participants in each group that were able to demonstrate a significant positive improvement in % correct up, down, and neutral moves over the course of training. Using the binomial distribution discussed in the next section and in Appendix A with a  $p=0.1$  level, 5 out of 12 participants in the ABS group is significantly different from chance ( $p<0.004$ ), while 1 out of 12 is not ( $p=0.718$ ).

### **Motor Learning Transfer.**

In order to assess whether or not participants were able to transfer the motor control they learned using EEG-BCI into improvements in their ability to physically perform the task, we measured the RMS error of the vertical distance between the cursor and the target bobbing on a moving sine-wave. Prior to any EEG-BCI training, each participant was asked to manually track the movement of the target with their finger five times. The RMS errors of each of these trials were recorded as the ‘before’ measures. After one hour of training and practice using the EEG-BCI, participants were again asked to physically track the movement of the target using their finger five times. The RMS errors of each of these trials constitute the ‘after’ measures. Comparing the RMS errors of the before and after measures gives us an indication of the amount of motor learning transfer that occurred due to the intervening practice that occurred between the before and after measures. An omnibus 2x3 ANOVA suggests that there is a significant difference before and after ( $F(1,66) = 13.16$ ,  $p < 0.001$ ) and a significant interaction between groups ( $F(2,66) = 4.702$ ,  $p = 0.01$ ). This is in direct support of Hypothesis H<sub>2a</sub> above. That is, if motor learning transfer occurs at all, the RMS errors before practice will be greater than the RMS errors after practice.

As a check against alpha inflation, Tukey’s HSD test was performed. Our F-scores exceed what would be required for alpha inflation to be a concern (HSD critical value = 3.55,  $F_{\text{before/after}}(1,66) = 13.16$ ,  $F_{\text{Interaction}}(2,66) = 4.7$ ) (Gravetter & Wallnau, 2011). Pairwise t-tests were performed to evaluate before and after differences in RMS errors. Table 3 shows the RMS error means of the before and after tests along with their associated p-values using one-tailed t-tests. We used a one-tailed t-test to compare the before and after RMS error of tracking performance assuming equal variances. We used the one-tailed test

because there is no evidence to support the notion that practicing a task would lead to poorer performance (Gravetter & Wallnau, 2000, p349). A smaller RMS error in the ‘After’ column supports that learning transfer has taken place. *P*-values less than 0.05 show that the learning transfer that occurred was significant.

None of the participants who practiced abstract imagery significantly ( $p < 0.05$ ) improved their performance on the manual task. The one significant slope was in the wrong direction, indicating their motor performance was worse after an hour of abstract imagery practice. In contrast, one third of participants who practiced embodied imagery significantly improved ( $p$  at a 0.05 criterion level) their performance in the manual task. Surprisingly, only two thirds (six with  $p$  at a 0.05 criterion level, plus two with  $p=0.057$ ) of participants who manually practiced the task for one hour significantly improved their performance in the physical task. The above is reflected in Figure 12 below.

The number of participants who improved their motor performance in each condition is shown in Figure 12. A simple equal probability sign test ( $p=0.5$ ), reveals that only in the manual practice condition were the number of participants who improved significant. However, when considering only those who improved to a  $p = 0.1$  criterion level, the number of participants who improved in both the manual and embodied imagery practice conditions were significant. The same is true when considering the number of participants who improved to a  $p=0.05$  criterion level. The number of participants who improved in the abstract imagery practice condition was not significant. Appendix A has a discussion on binomial distributions and shows the probabilities of the number of participants who should improve to different significance levels.



These findings are in direct support of hypothesis  $H_{2c}$  and are in direct contradiction to hypothesis  $H_{2e}$  discussed above. That is, the number of participants who demonstrated significant motor learning transfer (MLT), was greater for those practicing embodied imagery than for those practicing abstract imagery.

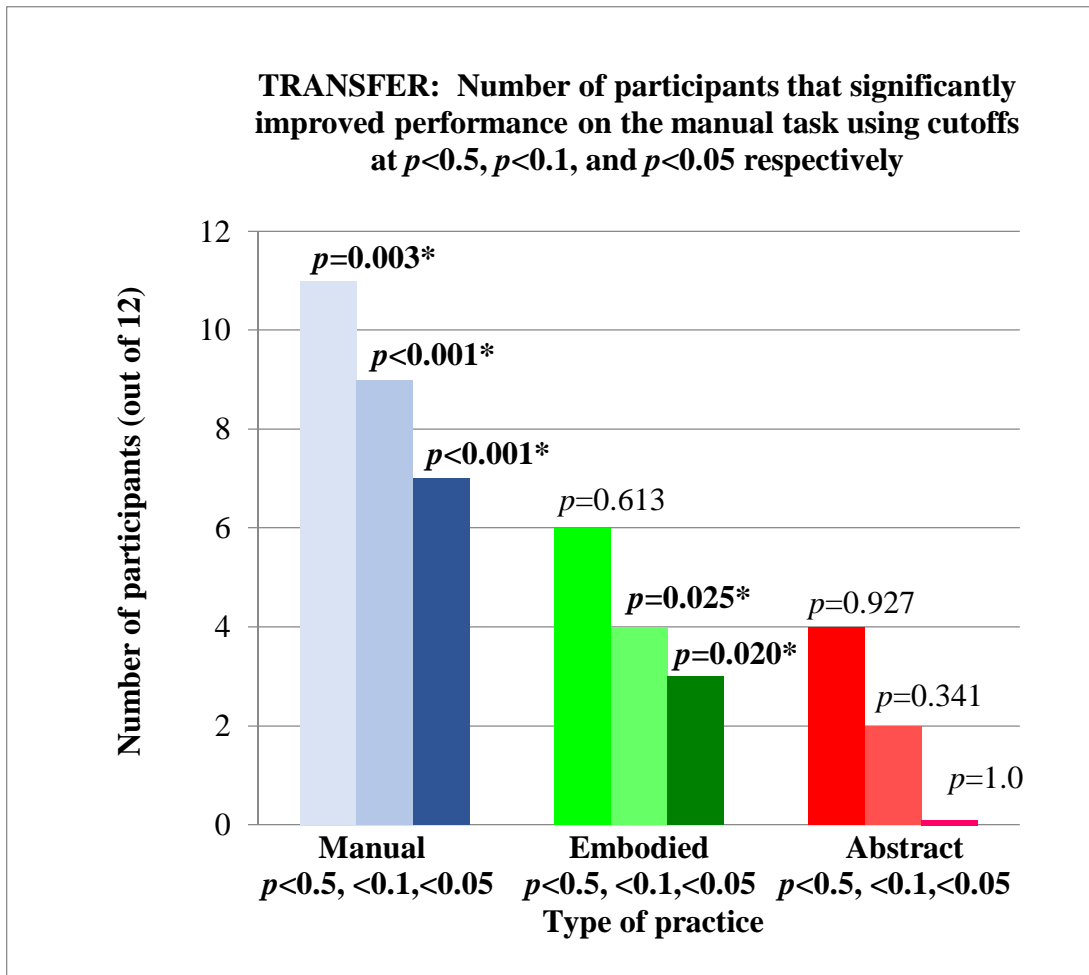


*Figure 12.* Evidence for motor learning transfer 1. The number of participants in each group that significantly improved their performance on the manual task after one hour of practice using cutoffs at  $p \leq 0.5$ ,  $p \leq 0.1$ , and  $p \leq 0.05$ , respectively. The p values listed above each column indicate the probability that that number of participants improved by chance alone. A simple sign test is done with a  $p \leq 0.5$ . Only in the manual practice condition is the number of participants who merely improved statistically different from chance. However, it is not likely that the number of participants who improved to the 0.1 and 0.5 levels occurred by chance in both the manual and embodied groups. The number of participants who improved in the abstract condition was not significant at any level.

Table 2.

One-tailed t-test comparisons of before and after mean RMS error of performance in the physical task. Tests are based on 5 before trials and 5 after trials. None of the participants who practiced abstract imagery improved their performance on the physical task at the  $p=0.5$  level. Red numbers indicate participants performed worse after practice. The one significant slope was in the wrong direction indicating the performance was worse after an hour of abstract imagery practice. One third of participants who practiced embodied imagery significantly improved their performance in the physical task. One half of participants (plus two more with  $p=0.057$ ) who actually practiced the physical task significantly improved their performance in the physical task (shown in bold blue).

Sub	Abstract		t-test <i>P</i>	Embodied		t-test <i>P</i> vals	Manual		t-test <i>P</i> vals
	Before	After		Before	After		Before	After	
1	39.624	40.094	0.4566	47.581	33.834	0.028	58.55	30.251	0.002
2	41.09	49.368	0.2316	49.407	47.305	0.407	47.052	39.457	0.105
3	44.599	44.020	0.4262	42.207	34.769	0.041	53.329	40.552	0.028
4	47.44	54.512	0.001*	40.701	36.600	0.127	87.104	70.374	0.141
5	53.24	45.612	0.0962	43.596	42.676	0.423	47.681	38.430	0.057
6	46.631	44.934	0.2633	59.899	41.835	0.046	53.004	33.029	0.000
7	56.264	50.555	0.1807	52.550	38.414	0.000	36.583	33.779	0.219
8	51.485	49.615	0.3632	41.209	39.100	0.305	61.090	33.547	0.000
9	48.59	44.847	0.3082	39.323	41.069	0.254	38.450	28.283	0.035
10	36.493	31.291	0.0621	41.216	40.039	0.309	45.611	25.555	0.000
11	34.532	30.801	0.1605	47.893	40.385	0.136	50.271	41.534	0.057
12	39.320	41.847	0.1023	38.856	43.897	0.084	65.977	34.743	0.007
Num Improved	7		0	10		4	12		7

Figure 13 (a) and (b) depicts two alternate ways of graphically representing motor learning transfer. Both (a) and (b) show the slopes of the manual task performance RMS error. Figure 13 (a) compares the before and after scores of each group so the slopes can be readily seen. Figure 13 (b) compares only the mean slopes of each group. That is, the mean slopes (averaged over all participants in each group) of the RMS errors before and after practice are significantly different for each of the three groups. The mean before and after RMS errors for the abstract condition were not significantly different from each other (one-tailed t-test,  $t(22) = .319, p = 0.376$ ). However, the mean before and after RMS errors for the embodied and the manual conditions were significantly different from each other (one-tailed t-tests,  $t(22) = 2.657, p = 0.007$  and ,  $t(22) = 3.16, p = 0.002$ , respectively). Combined, the above indicate that the reduction in RMS error in the embodied practice condition was significantly greater than the reduction in RMS error in the abstract condition. This is in direct support of Hypothesis H<sub>2b</sub> and in direct contradiction to Hypothesis H<sub>2d</sub> discussed above. In other words, those who practiced abstract imagery for an hour did not improve their manual performance, while those who practiced embodied imagery or manually practiced for an hour did improve their skill.

Tests were also done to compare the slopes of each condition to each other. A single factor ANOVA performed on all the slopes indicates a significant difference ( $F(2,33) = p < 0.001$ ). Again using one-tailed t-tests to compare each pair of conditions individually also suggests they are all significantly different from one another (abstract vs. manual:  $t(22) = 5.072, p < 0.001$ ; embodied vs. manual:  $t(22) = 3.25, p = 0.002$ . and finally, abstract vs. embodied:  $t(22) = 1.929, p = 0.0334$ ). Again, these findings support the notion that each type of practice conferred different amounts of motor learning transference to the

participants. Those who manually practiced showed the greatest improvement. Those who practiced embodied imagery showed a moderate amount of improvement. Finally, those who practiced abstract imagery showed no improvement at all.

The amount of transfer in each group was consistent with hypothesis H<sub>3</sub> discussed above. Namely, the amount of MLT was greatest for the manual practice group, followed by the embodied imagery group, followed by the abstract imagery group.

Our only way to assess the time required to learn EEG-BCI control was to use the time to first achieve 50% correct for each of the three types of moves. This was shown in Figure 9. There were no significant differences in the amount of time to reach 50% correct in each of the three types of moves between the embodied and abstract groups. This supports the null version of hypothesis H<sub>1b</sub>. That is, although the number of participants able to learn EEG-BCI control using abstract imagery was significantly greater than the number of participants who could learn EEG-BCI using embodied imagery, there was no significant differences between the two groups in the amount of time it took to learn EEG-BCI control for those who actually learned EEG-BCI control.

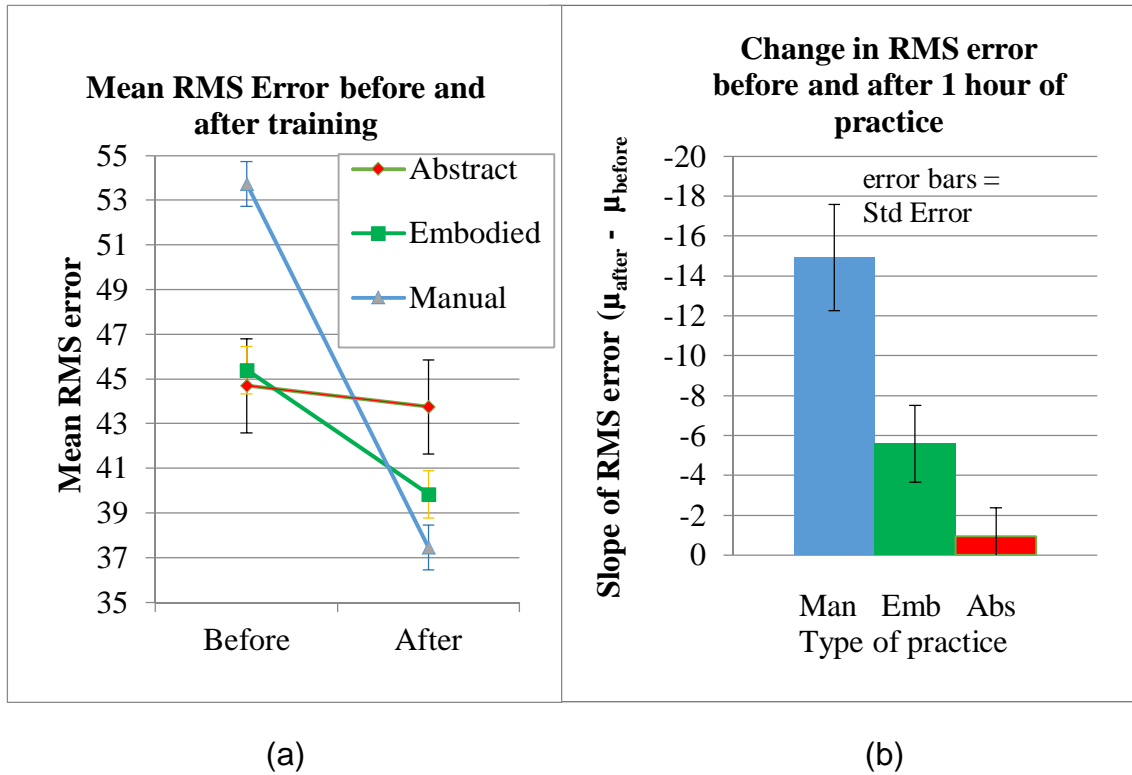


Figure 13. Evidence for motor learning transfer 2. Comparison of the before and after manual performance RMS errors between cursor position and target position. (a) The mean RMS error before and after practice. (b) The change in RMS error before and after practice. A single factor between groups ANOVA suggest all slopes are significantly different from one another ( $F(2,33)=14.42, p<0.001$ ). One-tailed t-tests to compare each pair of conditions suggests they are all significantly different from one another (abstract vs. manual:  $t(22)=5.07, p<0.001$ . embodied vs. manual:  $t(22)=3.25, p=0.002$ . and finally, abstract vs. embodied:  $t(22)=1.928, p=0.0334$ ).

## CHAPTER SEVEN

### DISCUSSION

#### **Motor Learning Transfer.**

Based on previous studies using embodied mental imagery (EMI), we expected that those who imagined moving their fingers and arms to move the cursor would also get better at physically moving the cursor with their arms. The negative slope in Figure 12 indicates that those who imagined moving their arms and finger up and down to control a cursor did, in fact, improve their ability to perform the physical task, although not as much as those who actually physically practiced the task. What was unclear was whether or not those who learned to move the cursor using abstract disembodied imagery would also improve their performance in the physical task. The absence of a significantly negative slope for those that used abstract imagery suggests that they did not improve their ability to perform the physical task. Moreover, no member of the abstract group significantly improved their performance of the manual task even after an hour of practice with abstract imagery, yet one third of the embodied imagery group along with two thirds of the manual group did show improvement after an hour of practice. There is a clear difference in motor learning transfer when abstract imagery vs. embodied imagery is practiced.

The results suggest that the group who used abstract disembodied imagery did not transfer their skills into the performance of the physical task (i.e. the before and after RMS errors were not significantly different ( $\Delta\text{RMS} = 0.94$  pixels; one-tailed t-test,  $t(22)=.319$ ,  $p = 0.376$ , Cohen's  $d=0.529$ ). The results also suggest that the group who practiced embodied imagery did demonstrate motor learning transfer to the physical task (i.e. the

before and after RMS errors were significantly different; ( $\Delta$ RMS = 5.57 pixels; one-tailed t-test one tailed,  $t(22)=2.647$ ,  $p= 0.007$ , Cohen's  $d=1.098$ ).

Together, these findings go against Paivio's (1986) suggestion that performance improvements after mental imagery practice might simply be due to motivational factors such increased arousal and attention. In the EEG-BCI task, more participants who used abstract imagery learned to control the cursor than those who used embodied imagery (Figure 8). Clearly then, the abstract group was at least as motivated as the embodied group, yet they showed no motor learning transfer to the physical task. The embodied group did show motor learning transfer. These findings support Decety's (1996) and Yaguez's (1998) contention that the transfer of motor learning is due to the fact that the same neural structures which are used in embodied imagery are also the structures that are involved in the actual motor execution of the imagined act. Our experimental design, however, was not able to address the original concerns expressed by Paivio and others. That is, we do not attempt to explain why motor learning transfers to non-homologous musculature.

### **Abstract Imagery May Be Better For EEG-BCI Control.**

It was originally thought that EEG signals derived from abstract disembodied imagery would be easier to differentiate than EEG signals derived from embodied imagery because abstract imagery may be more distributed throughout the brain than motor imagery. Although there was no statistically significant difference in the number of participants in the embodied and abstract groups who could reach the 50 % correct criteria in the time allotted, trend analysis revealed something quite different. Trend analysis showed that while 41.7% of those using abstract imagery were able to learn EEG-BCI



control, only 8.3% of those using embodied were able to do so. There was considerable difference in the number of participants who showed improvement in the EEG-BCI task over time between the two groups. It seems therefore, that it is easier to learn EEG-BCI control using abstract imagery than embodied imagery.

It may be that the relevant EEG signals for abstract representations may be more widespread over the skull than those involved in hand and finger movements. Miller (2010) showed that both imagery and movement of the hand excited similar area in the frontal cortical areas. Lamm, et al. (2007) showed that mental rotation excited large areas of the parietal cortex. Additionally, Lehmann et al. (2010) demonstrated that discrete nouns with high and low imageability (e.g. “table” vs. “gist”) highlighted posterior and frontal temporal lobes respectively. If the above is true, then it may be that abstract imagery, and/or embodied imagery, along with mental rotations may be useful manipulations for optimizing control with EEG BCI apparatus. It is good to keep these concepts in mind when designing EEG-BCI apparatus targeted at those with disabilities. A person with ALS, for example, may find it beneficial to use abstract imagery for EEG-BCI control. Learning transfer to physical movements are likely to be of little use due to the degenerative nature of the neuromuscular disease. A stroke patient who hopes to regain some control of the paralytic limb, however, may be better off learning to control the EEG-BCI using embodied imagery. Even if it is more difficult to learn, the potential for motor learning transfer may justify the extra effort.

**SECTION 2:**  
**ARTIFICIAL NEURAL NETWORK FOR EEG SIGNAL PROCESSING**  
**CHAPTER EIGHT**

**INTRODUCTION**

It is unsatisfying that this research required the use of proprietary signal analysis software to map the output of the 14 EEG electrodes onto the up/down/neutral cursor control signals. In addition, the proprietary decoding algorithm does not improve over time. Once the machine is calibrated, the parameters are set. Short of recalibration, the best the user can do is learn to repeat the EEG patterns he or she produced during calibration. This calibration first, control later approach has been used by others for EEG-BCI based control (Bradberry, et al., 2011). In the following section we will explore an alternative approach that uses a back propagation artificial neural network to better map the power spectrum of EEG signals into machine commands. Using a neural network that can learn from experience will make possible EEG-BCI control applications that adapt to users and improve over time. This is an important consideration because temporal and spatial changes which occur in the brain during learning will likely alter EEG patterns as well (Driemeyer et al., 2008). Our alternative open-source method of EEG-BCI control can be configured to adapt to users over time in future applications.

**Artificial Neural Network Basics.**

Artificial Neural Networks (ANNs) are really nothing more than a collection of massively interconnected processing elements assembled in various ways. In a typical ANN, the processing elements (also called units or “Neurons”) are organized into layers

such that each neuron in one layer is connected to every neuron in the next layer (see Figure 13). The input to each neuron is either from the environment (in the first layer), or the sum of all the activation levels of each neuron in the immediately preceding layer multiplied by the strength of the connections between them ( $\text{Input}_j = \sum A_i W_{ij}$ ). The output of each neuron is usually a non-linear function of the sum of all its inputs. We used the  $\tanh(x)$  sigmoid function shown in Figure 14. The sigmoid function is a squashing function which limits the output so that it ranges between negative and positive one. When the sum of inputs is a large positive number, the neural output is one; when the sum of inputs is a large negative number, the neural output is negative one. The sigmoid activation function increases the probability that each neuron will be in a state somewhere between negative and positive one.

The beauty of these types of networks is that the connection strengths between each neuron can be gradually adjusted so that a set of inputs can be mapped into a set of desired outputs. The gradual adjustment of the strengths of the interconnections between neurons so as to create mapping from inputs to desired outputs is loosely referred to as “learning” in an ANN. There are many possible learning algorithms available to train ANNs. Here we will use a basic back-propagation algorithm (Rumelhart et al., 1995). In back-propagation, the actual output is compared to some desired output. Then the error is used to adjust the weights backwards through the net such that:

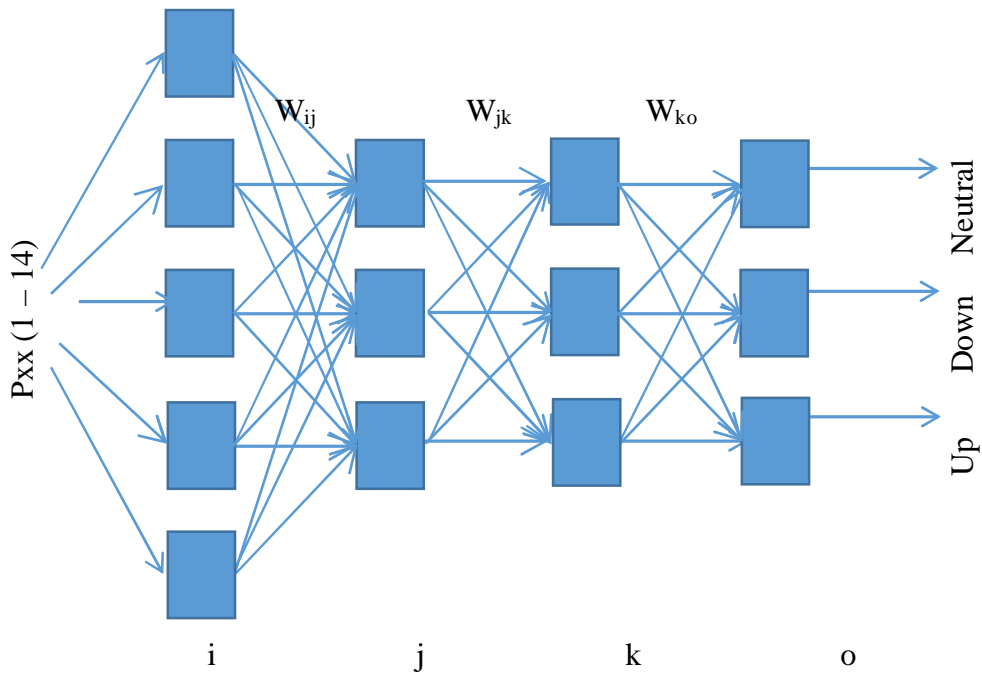
$$w\Delta w = -\alpha \frac{dE}{dw(t)} \quad (11)$$

Where:

$\frac{dE}{dw(t)}$  is the derivative (slope) of the error E at time t (in epochs)

$\alpha$  is the learning rate

Essentially, this becomes a gradient descent function in a hyperspace of all possible weights. There is always a danger that the network will find a local minimum in that space and not be able to continue its descent into the most optimum solution. Variable learning rates and a momentum term help ameliorate this situation. These issues will be discussed further in the network architecture section.



$$\text{Input}_i = P_{xx}$$

$$A_j = \sum \text{Input}_i W_{ij}$$

$$A_k = \sum A_j W_{jk}$$

$$\text{Output}_o = \sum A_k W_{ko}$$

Where:

$A = \text{sigmoid}(\text{input}) = \text{Activation of a given neuron}$

Each square represents a processing element or “neuron”.

*Figure 14.* Basic ANN architecture. Each electrode provides inputs to 20 neurons using the 4x5  $P_{xx}$  power matrix generated as described in the text. Together, the 14 electrodes provide inputs to 280 neurons in layer (i). Neural layer (j) and (k) are hidden layers. Layer (o) is the output layer. There are three output neurons and only one is active at a time. One represents an up command, another the down command, and the last the neutral command.

### Sigmoid function

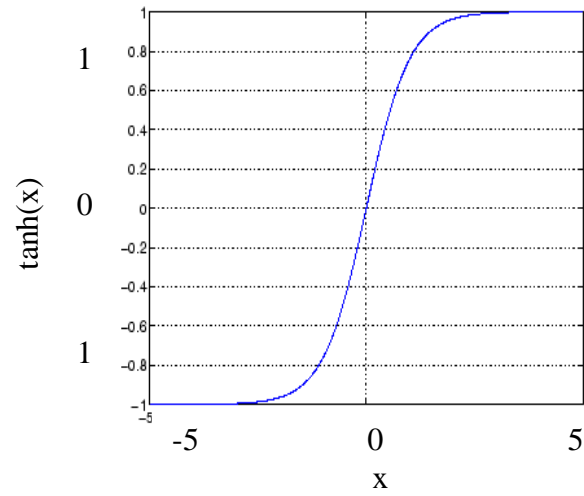


*Figure 15.* The  $\tanh(x)$  function. Note the output is bounded by -1.0 and 1.0 as  $x$  ranges from  $-\infty$  to  $+\infty$ . Note that this is a non-linear function as opposed to linear models most often used in psychology today.

## **EEG-BCI Artificial Neural Network Inputs.**

Our goal here is to map a set of EEG signals into one of three output commands: up, down, and neutral. It is evident from Figures 2 and 3 in Chapter 3, that raw EEG signals may be difficult to interpret. To pull out relevant information from the raw EEG data, we first create a spectrogram of the incoming signals by taking short time interval fast Fourier transforms (SFFTs) of the data. I will not go into the mathematics of Fourier here as they well covered elsewhere (Cerna and Harvey, 2000). However, I will demonstrate their usefulness in the discussion that follows. Figure 16 shows a spectrogram made using the SFFTs. The x-axis represents time. The vertical axis shows frequency. The color indicates the power (or rate of energy transferred in Joules/s) of the different frequencies at specific time windows (red is relatively higher power than blue). The power is negative because we are looking at EEG signals backwards in time from the moment the command is received. The information in figures like this will be used as inputs into an artificial neural network used to map EEG data into machine commands.

Underlying the colorful figure is really a matrix of power values,  $P_{xx}$ , whose size is the number of time bins by the number of frequency bins. The spectrogram functions smears the colors (here representing the power at a particular frequency and time) over the range of the  $P_{xx}$  time and frequency bins. The values of the  $P_{xx}$  matrix are better represented using a radial basis function (Rbf) around the power values. We further simplified the  $P_{xx}$  matrix by scaling the power values so that they range from zero to one. The resulting  $P_{xx}$  power matrix is shown in Figure 17. The scaling of the  $P_{xx}$  values is performed as follows:

$$\text{NewPxx}(i, j) = \frac{\text{Pxx}(i, j) - \text{MinPxx}}{(\text{MaxPxx} - \text{MinPxx})} \quad (12)$$

The SFFTs allow us to retain some of the time information in the data. The length of the time window and the amount of overlap between each window used for the FFT affect the frequency and time resolutions that are possible from a given set of EEG inputs. As the length of the time windows are increased, the frequency resolution is increased at the expense of the time resolution. On the other hand, a shorter time window improves the time resolution at the expense of frequency resolution (lower frequencies disappear in shorter time windows). We need a compromise between the length of the time and frequency resolutions we wish to resolve. But first we must explore the specifications of the EEG equipment.

The EPOC<sup>®</sup> headset samples each electrode at 128 samples per second. That is a sample every  $1/128 = 7.8$  ms. EPOC<sup>®</sup> recommends polling for new commands 10 times per second (or every 100 ms). Therefore each sample of user intention is based on 12 separate EEG readings of each of the 14 electrodes (i.e.  $100/7.8 = 12.8$ ). The maximum frequency we can detect at this sampling rate is defined by the Nyquist criteria (Cerna and Harvey, 2000),  $f_{\max} = 1/(2i)$ , where  $i$  indicates the sampling interval. The maximum frequency we can hope to detect is 64Hz (i.e.  $1/2(0.0078) = 64.1$ ).



Power Spectrograms: training “down”;  
Hanning Window; NFFT=8; Overlaps = 6; pad to 16  
P7

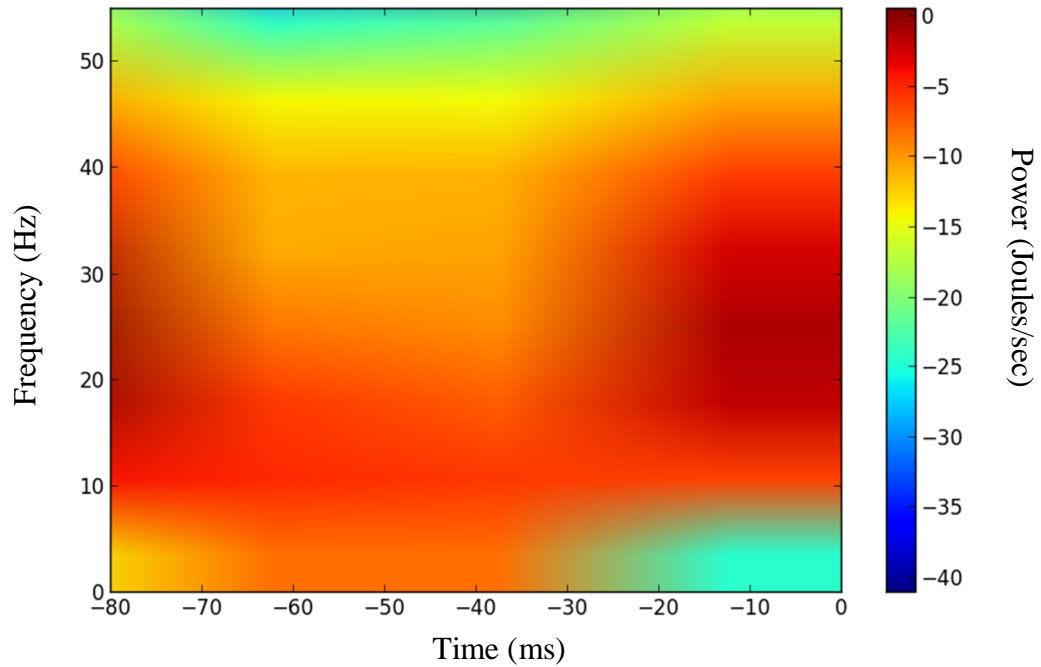


*Figure 16.* Power spectrogram of electrode P7 while the participant was imagining moving the cursor down with her arm and finger. Note that at time 0, the data packet is received. EEG data occurs prior to command. The power values are negative because we are looking backwards in time.

Power Spectrograms: training “down”;  
Hanning Window; NFFT=8; Overlaps = 6; pad to 16  
P7

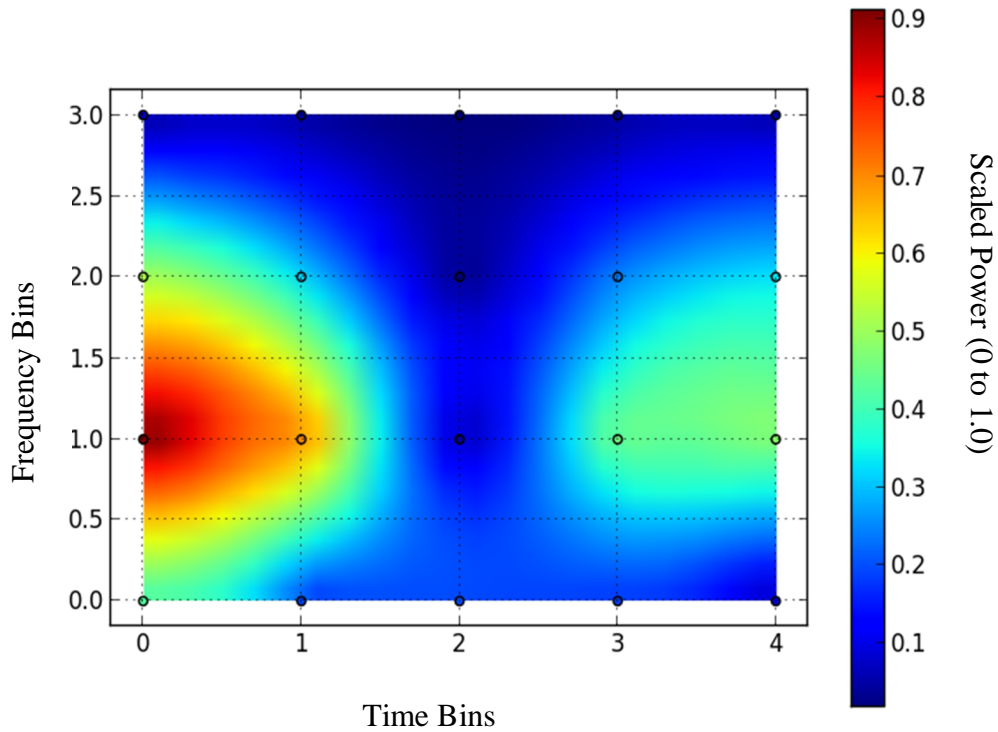


*Figure 17.* Power spectrum viewed through radial basis function. Power matrix values plotted with a radial basis function to reduce the color smear of overlapping windows of electrode P7. Participant was imagining moving the cursor down with her arm and finger. Power has been scaled so that it ranges from zero to 1.0. Axes reflect row and column of Pxx matrix.

In addition to sampling rate, we must also determine the number of samples needed. National Instruments, Inc. suggests a minimum of 3 cycles need to be sampled for proper frequency identification (Cerna and Harvey, 2000). Since we are sampling twice as fast (128 Hz) as the maximum signal frequency that can be detected (64 Hz), and we need to sample for a minimum of three cycles, we need at least 6 data points ( $6 = (2 \text{ samples/cycle}) \times 3 \text{ cycles}$ ). We used 8 data points for each SFFT calculation.

Although EPOC<sup>®</sup> recommends polling for new commands every 100ms, in reality, commands are sent only when a command was recognized. Data packets are only transmitted when there is a corresponding command. As a result, the data packets that arrive at the host computer may be of different lengths, and may arrive at times varying from the suggested 100ms polling interval. To ensure a consistent number of samples, a record is kept of preceding EEG values. The appropriate number of these records are tacked on to the back end of each data packet to ensure a consistent number of samples for each set of SFFTs calculations. Although the packets are discrete and of inconsistent length, stitching together data from multiple packets assures that we are getting consistent and continuous EEG signals.

SFFTs were calculated using a window of eight data samples sliding over a total of 16 data points. Each successive SFFT calculation overlapped the previous by six samples. Figure 18 shows that five 8 data point windows can be fitted into 16 data points when each window overlaps the previous by 6 points. The time of each of these windows is known relative to the time the data packet was received. Each SFFT transformation is performed over each time window. Although an FFT transformation loses the time information, the five small windows provide five time bins which allow us to retain a record of time. We

wanted at least 5 time bins, so elected to use a moving record of 16 data points from each electrode.

The shape of the sliding window affects the spectral estimate computed with the SFFTs. We used a Hanning window because it is commonly used in narrow band applications (Cerna & Harvey, 2000).

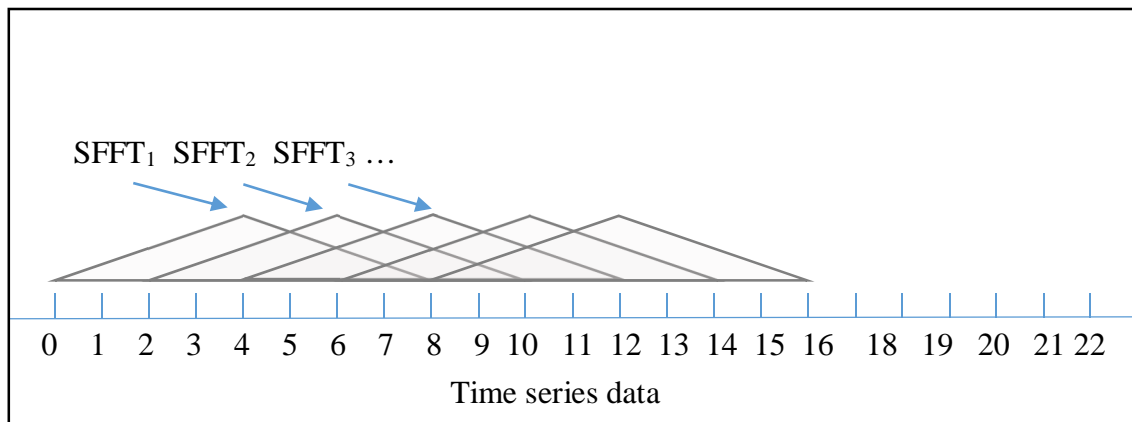


*Figure 18.* Graphical depiction of SFFT. Each SFFT is computed using an 8 data point window. The data window of each subsequent SFFT overlaps the previous by 6 data points. The SFFT window evaluated the power of each frequency band at a particular time. With a window of 8 data points, 5 time windows are possible. Note that the centers between each time window are two data points apart. When sampled every 7.8 ms, our time resolution is 15 ms. The triangle is for illustrative purposes only, we used a Hanning window (see text)

Figures 19-21 show spectrograms of the SFFTs taken from the voltage values of each electrode over approximately 100 ms time intervals. Each plot contains both time and frequency distributions, as well as the power (color) contained in each time and frequency bin. The image is generated from a power matrix ( $P_{xx}$ ) obtained when the SFFTs are

calculated within each time window. The number of time bins (in our case 5), the number of frequency bins (in our case 8), and the amount of window overlap (in our case 6) determine the dimensions of the Pxx matrix. The power matrix and associated spectrogram images reflect differences which may be exploited to generate desired output commands.

Each element of the power matrix (Pxx) provides the input to the single neuron in the ANN. Each ANN input neuron contains the mean power of the EEG signal for about 15.6 ms and frequencies that span about 8 Hz.

We elected to turn the 8x5 spectrogram from each electrode into a 4x5 set of inputs to reduce the number of input neurons to a total of 280 ( $4 \times 5 \times 14 = 280$ ). This reduction in inputs was accomplished by averaging every two rows in the Pxx matrix, thus reducing the number of rows by two. Each frequency bin now spans 16 Hz.

**Power Spectrograms through RB function: Training  
“DOWN”; Hanning window; NFFT = 8; Padded to 16**

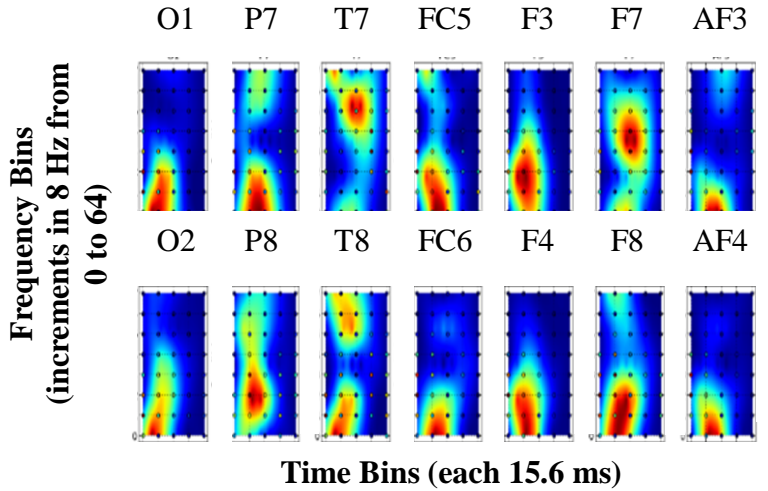


Figure 19. Spectrograms of short time interval FFTs for each electrode of a participant contemplating an abstract concept that has been mapped to the down command. The x-axis shows time bins. The vertical axis shows frequency. The color indicates the power scaled so that it is between 0 and 1.

**Power Spectrograms through RB function: Training  
“UP”; Hanning window; NFFT = 8; Padded to 16**

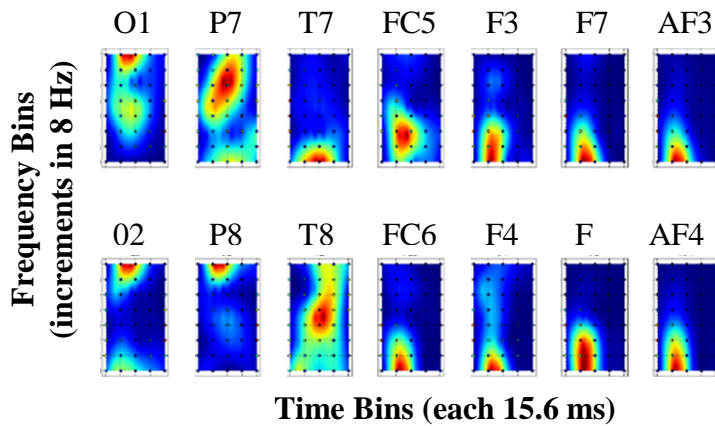
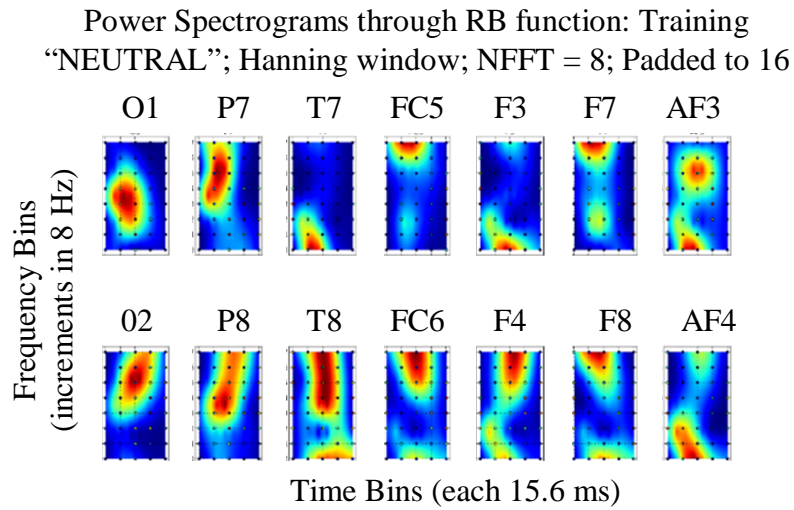


Figure 20. Spectrograms of short time interval FFTs for each electrode of a participant contemplating an abstract concept that has been associated with the up command. The x-axis shows time bins. The vertical axis shows frequency. The color indicates the power which has been scaled so that it is between 0 and 1.



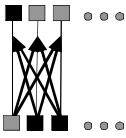
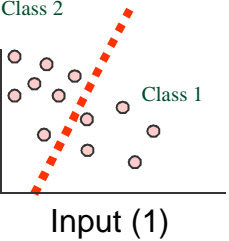
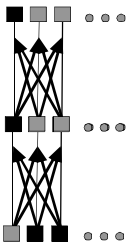
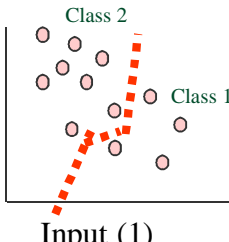
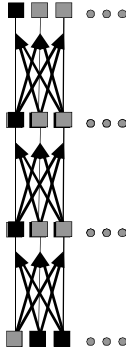
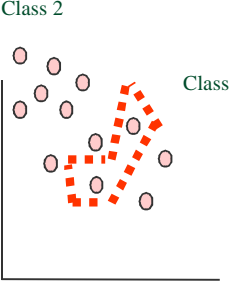
*Figure 21.* Spectrograms of short time interval FFTs for each electrode of a participant contemplating an abstract concept that has been associated with the neutral command. The x-axis shows time bins. The vertical axis shows frequency. The color indicates the power which has been scaled so that it is between 0 and 1.

### **Network Architecture.**

There are many other possible interconnection architectures, but here we will only consider a feed-forward four layer network described below. The number of layers in a feed-forward network determines the range of data that can be mapped into desired outputs. Lipman (1987) showed that the number of hidden layers can impact the level of processing possible on a given data set. For example, suppose we have a network with only two inputs and two outputs. The two inputs represent two distinct features of some class of objects. The two output units represent the two categories of objects the network is trying to classify. Such a network, without any hidden layers, can only linearly separate a feature space into two sections (See Table 4). A single intermittent layer between the input and output layers allows the network to perform more complex classification tasks (Lipman, 1987) . Two intermittent layers allows for an arbitrary segmentation of an input space into an arbitrary output space. We therefore elected to use two hidden layers in our network.



Table 3.  
*Processing ability as function of hidden layers.*

<p>Num. Hidden Layers</p> <p>0</p>	<p>Output Layer (k)</p> <p>Weights (j, k)</p> <p>Input Layer (i)</p> 	
<p>1</p>	<p>Output Layer (k)</p> <p>Weights (j, k)</p> <p>Hidden Layer (j)</p> <p>Weights (i, j)</p> <p>Input Layer (i)</p> 	
<p>2</p>	<p>Output Layer (n)</p> <p>Weights (m, n)</p> <p>Hidden Layer 2 (m)</p> <p>Weights (j, k)</p> <p>Hidden Layer 1 (j)</p> <p>Weights (i, j)</p> <p>Input Layer (i)</p> 	

Another consideration is the number of neurons in each processing layer. Too few neurons and the network will not learn. It turns out that it is easier to train networks with excessive number of neurons. However, more neurons than necessary may cause overfitting which leads to poor generalization to untrained examples (Hunter et al., 2012).

Other considerations include the learning rate, the minimum error tolerated, the momentum, and the level of activation of the target values. The performance of a backpropagation error correction algorithm is very sensitive to the learning rate. If too large, the network may oscillate and never settle to minimum error. If too small, then it may take too long to settle on a good set of weights. Variable learning rates often improve convergence rates (Danilo and Chambers, 2000). The momentum term is not part of the gradient descent per se, but is merely a heuristic that reduces oscillations and increases learning speed (Rumelhart et al., 1986). The minimum error tolerated is used to stop the learning process. It is basically a “good enough” heuristic. The level of activation of the target is set to 0.7 (instead of 1.0) so that the network can err on either side. It is just another heuristic that seems to improve performance, perhaps because it prevents overlearning. To arrive at a suitable combination of parameters, as well as to determine the optimum number of neurons in the middle layers, we used a trial and error method that can be followed in Table 5.

Table 5 shows our meandering search for a suitable combination of parameters. Each row in the table represents a trial. Red numbers indicate which parameters were changed in a given trial. Green values represent the best parameter choices. The top part of the table represents trials where about 100 examples of EEG signals for up, down, and neutral imagery. The number of examples are doubled in the lower part of the table. The

last column in Table 5 shows each network's performance (% correct) under various parameter changes. Note that the largest number of neurons does not necessarily produce the best performance.

Another reason to limit the number of neurons in the network is that the number of calculations required to propagate inputs through the network increases exponentially with the number of neurons. A 3x3 neural arrangement has 9 interconnections. Propagating across this network requires:  $3(9)=27$  calculations. Doubling the number of neurons so that it is a 6x3, creates 18 connections, requiring  $6(18)=108$  calculations. The situation is worse in a four layer network. It is desirable, therefore, to keep the number of neurons at a minimum.

After the various iterations shown in Table 5, we settled on a 280x10x5x3 network configuration, with a maximum allowed error of 0.015, a learning rate of 0.007, and a momentum of 0.3. In the bottom of the table, we also list a few runs with identical configurations, but doubled the number of examples used during training. No advantage was found to doubling the number of examples, a troubling observation that will prove instructive later on in this discussion. Let us now look at how this network performs on data from other participants.

Table 4.

*Trial and error parameter selection.* Each row in the table represents a trial. Red numbers indicate which parameters were changed in a given trial. Green values represent the best parameter choices. The top part of the table represents trials where about 100 examples of EEG signals for up, down, and neutral imagery. The number of examples are doubled in the lower part of the table. No improvement is noted with more examples.

TRAINING SET SIZE (Up, Down, Neutral): 101, 101, 114									
Number of neurons				Variable parameters			Training Stats		%
In	Lyr (j)	Lyr (k)	Out	ErrMax	L.R.	M.	Cycles	Time(s)	Correct
280	7	3	3	0.025	0.01	0.3	75	171	37.28
280	7	4	3	0.025	0.01	0.3	68	154	39.22
280	7	5	3	0.025	0.01	0.3	61	141	37.62
280	10	4	3	0.025	0.01	0.3	65	209	38.04
280	10	5	3	0.025	0.01	0.3	53	181	39.90
280	10	6	3	0.025	0.01	0.3	53	177	37.79
280	10	5	3	0.025	0.02	0.3	399+		
280	10	5	3	0.025	0.005	0.3	53	169	39.56
280	10	5	3	0.025	0.015	0.3	53	169	39.64
280	10	5	3	0.025	0.007	0.3	53	168	39.90
280	10	5	3	0.025	0.008	0.3	53	169	39.81
280	10	5	3	0.025	0.0075	0.3	53	168	39.81
280	10	5	3	0.025	0.007	0.4	49	160	38.80
280	10	5	3	0.025	0.007	0.2	69	218	38.80
280	10	4	3	0.025	0.007	0.2	72	231	38.12
280	12	5	3	0.025	0.007	0.2	63	242	37.79
280	7	4	3	0.025	0.007	0.3	68	160	38.88
<b>280</b>	<b>10</b>	<b>5</b>	<b>3</b>	<b>0.025</b>	<b>0.007</b>	<b>0.3</b>	<b>60</b>	<b>195</b>	<b>40.83</b>
280	7	4	3	.1-.015	.2-.007	0.3	71	154	37.7
280	10	5	3	.1-.015	.2-.007	0.3	71	218	38.29
280	10	5	3	.1-.015	.2-.007	0.3	71	224	38.21
<b>280</b>	<b>20</b>	<b>5</b>	<b>3</b>	<b>.1-.015</b>	<b>.2-.007</b>	<b>0.3</b>	<b>56</b>	<b>328</b>	<b>40.83</b>
280	50	5	3	.1-.015	.2-.007	0.3	54	900	38.46
280	10	10	3	.1-.015	.2-.007	0.3	68	223	37.95
280	100	50	3						
280	160	70	3						
TRAINING SET SIZE (Up, Down, Neutral): 191, 191, 186									
Number of neurons				Variable parameters			Training Stats		%
In	Lyr (j)	Lyr (k)	Out	ErrMax	L.R.	M.	Cycles	Time(s)	Correct
280	10	5	3	0.015	0.007	0.3	75	443	39.15
280	10	5	3	.1-.015	.2-.007	0.3	103	573	36.44

### **Artificial Neural Network Performance.**

Figure 22 (a) and (b) compare the ANN's performance to that of the EPOC<sup>®</sup> apparatus. Although our ANN shows evidence of learning and generalization, its performance is not very impressive. Given that neural networks have been successfully used in fault tolerant situations in pattern recognition and machine control (Deora and Bajaj, 2012; Estrera et al., 2012; Yin et al., 2012, Singh, 2012), it is surprising that our network did not perform better. Clearly the network was able to correctly map the EEG patterns in the training sets, but only slightly better than chance on untrained patterns. Although other network training algorithms are possible which reduce the probability of finding a local minimum in the solution space, we used a simple error back-propagation network for our task because these other algorithms are not well suited for large networks. We used the minimum processing units possible to improve generalization (Wilamowski and Yu, 2010).

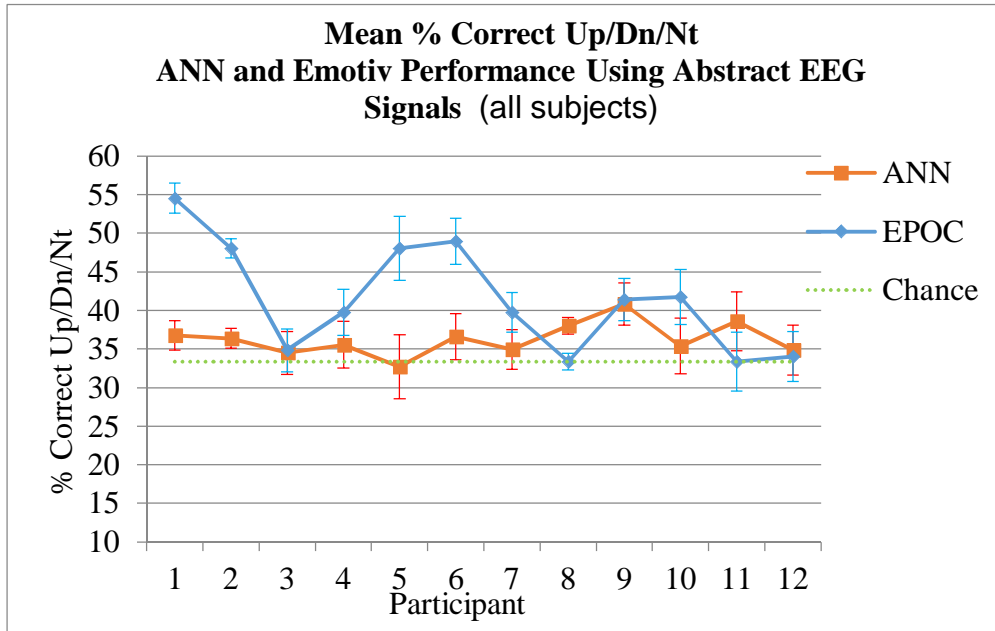
The fact that performance was poor and that doubling the number of examples did not improve the ANN's performance suggests that we may have bad examples. The importance of good training examples cannot be overstated.

Imagine learning numbers for the first time when given erroneous information even a small percentage of the time. Figure 23 illustrates this analogy. Suppose the first three figures in the top row are given as examples of the number two. A consistent mapping would be difficult especially when later given examples of the number three. However, when averaged together (as in the fourth figure in the top row), the erroneous image of the number three gets lost in the averaging process. This single averaged example of a number

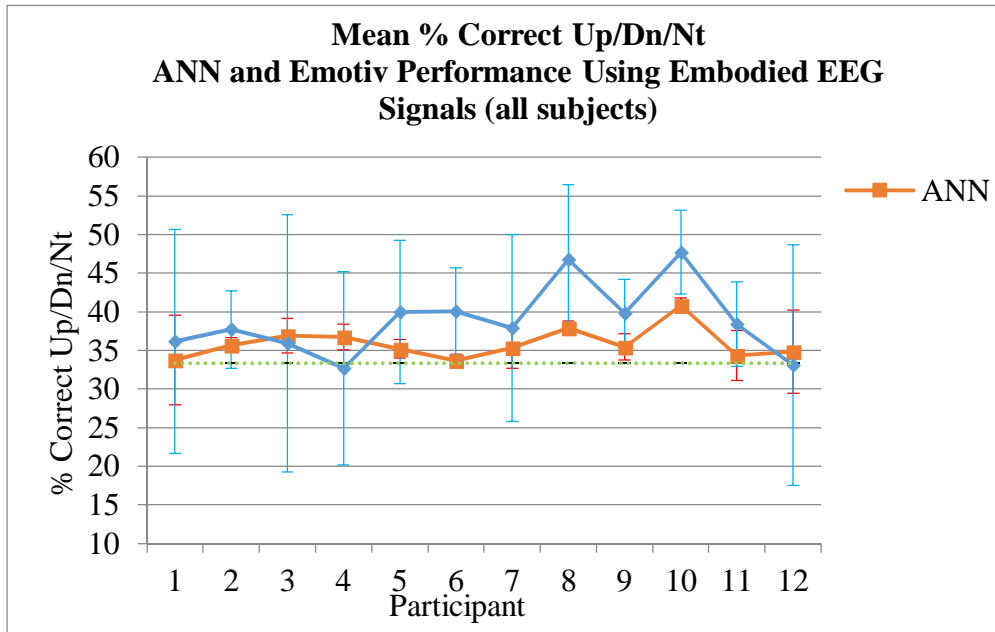
two is less likely to cause problems than the three separate examples containing fallacious data. Of course, the above presumes that good examples are predominant in the data.

Our training set probably suffers from the same vagaries. Just because the training program prompts the participant to imagine moving “UP”, or some pre-agreed-to abstract concept, does not necessarily assure us that the participant is in fact doing so every 124 ms ( $7.8 \times 16 = 124$  ms). Our training set could be replete with bogus EEG signals from distracted participants. There are several options for dealing with this issue. Most require the collection of additional data and each will be discussed below in the discussion section. However, using only existing data, one could average the EEG data from several consecutive commands. In doing so, “bad” EEG data would be averaged in with “good” data so that errors would tend to “wash” out. Data averaging in this way would reduce the chances that the learning algorithm would be led astray by erroneous data. To be clear, the Pxx matrix for each electrode was averaged over seven consecutive trials before it was used as a training example, not the raw EEG data.

Figure 24 shows the ANN’s performance when seven consecutive data packets for a given command are averaged and used as single training example. This is not the same as increasing the number of examples. Rather, it ensures that bad examples are averaged in with good examples so that they are no longer used as individual training trials. The ANN’s performance using data averaging is compared with EPOC<sup>®</sup> performance in the next section. EPOC performance has been rank ordered from best to worst. Note that the ANN performance (in terms of percent correct) is in fact, negatively correlated to the performance of the EPOC algorithm (corr= -0.1325 and corr = -0.4325 for abstract and embodied respectively).

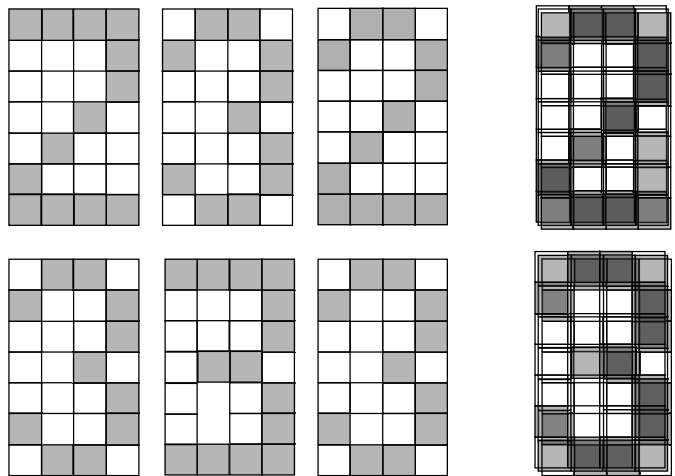


(a)



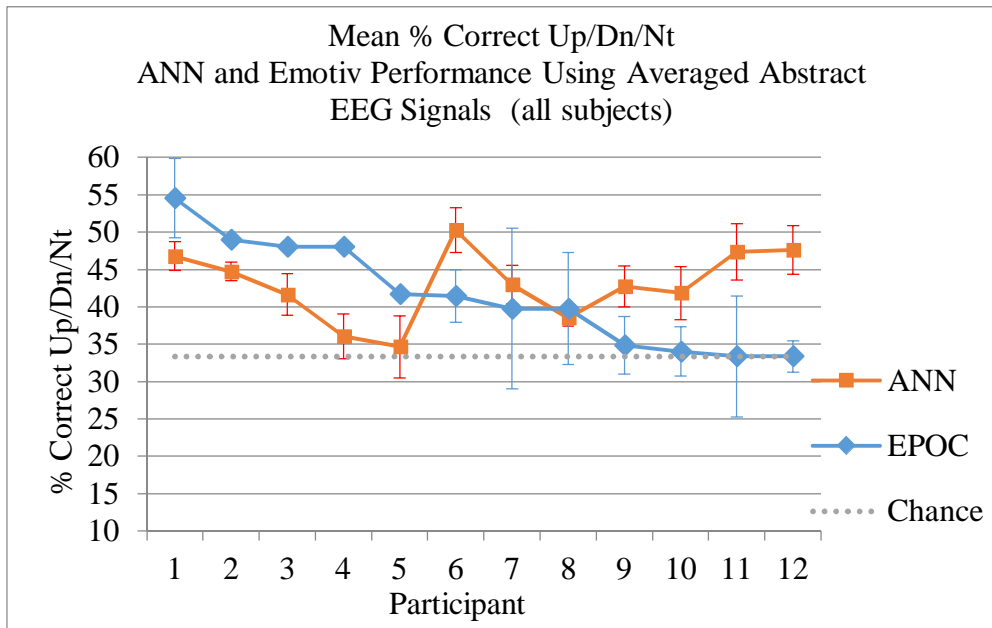
(b)

Figure 22. Performance of ANN in generating proper up, down, and neutral commands. (a) EEG generated from abstract imagery. (b) EEG generated using embodied imagery. Error bars are standard errors.

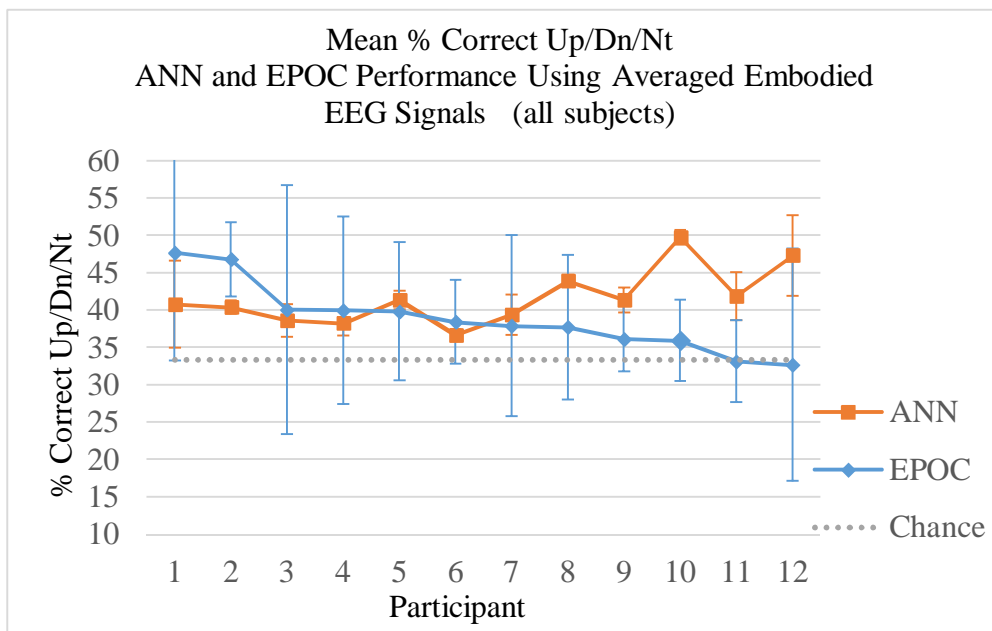


*Figure 23.* Averaging training samples. Illustration of the concept of averaging examples to reduce the deleterious effects of bad exemplars. Note that if the number three were given as an example of a two, confusion could result. But if the examples of twos were averaged, the negative effects of the bad example is minimized (see averaged examples in last column above).





(a)



(b)

Figure 24. Performance of ANN in generating proper up, down, and neutral commands when every 7 input Pxx matrices were averaged prior to propagation through network. The %Correct are rank ordered by the EPOC group. (a) EEG generated from abstract imagery. (b) EEG generated using embodied imagery. Error bars are standard errors.

### **Network Performance with Data Averaging.**

The following discussion concerns only the ANN's performance when using data averaging. There was no significant difference between the overall performance of the ANN and the EPOC<sup>®</sup> in the abstract condition (two-tailed t-test,  $t(19)=0.587$ ,  $p = 0.564$ ). There was also no significant difference between the overall performance of the ANN and the EPOC<sup>®</sup> in the embodied condition (two-tailed t-test,  $t(21)=1.611$ ;  $p = 0.122$ ). There was, however, a significant difference between ANN performance and chance for both the abstract and embodied condition (two-tailed t-test,  $t(11)=6.946$ ;  $p<0.001$  and  $t(11)=7.601$ ;  $p<0.001$ , respectively). That is, our ANN was an effective means of mapping user intentions into machine commands and it was as effective as the EPOC<sup>®</sup> proprietary algorithm. Interestingly, the standard errors of the ANN percent correct performance are considerably smaller than those of the EPOC (two-tailed t-tests,  $t(22)= -2.117$   $p<0.045$  for abstract, and  $t(22)= -2.527$   $p<0.019$  for embodied). This indicates that its performance on up, down, and neutral moves were close to each other. That is, roughly the same percent correct for each type of move. That is not so for the EPOC<sup>®</sup>, where the high standard errors indicate that good performance on a particular command sacrifices performance on another. For instance, it may do well on up commands, but not so well in neutral commands. Visual inspection of Figure 23 (a) and (b) further, suggests that the participants who performed well with the EPOC<sup>®</sup>, are not necessarily the same participants who performed well using the ANN. In fact, the performance of the ANN is negatively correlated to the performance of the EPOC. This observation suggests that our ANN utilizing averaged power matrices calculated from SFFTs as inputs is a fundamentally different approach from the proprietary one used by EPOC<sup>®</sup>. The fact that the performance

of two mapping algorithms can be inversely correlated suggests that further exploration of relevant EEG signal features is warranted.

We have stressed the importance of an error free training set and demonstrated the use of data averaging to improve the performance of the ANN in the previous section. Here we will now suggest other approaches to improving the quality of the training set. These have not yet been explored because they will require the acquisition of additional data sets.

One possibility for assuring the quality of the training data set is to give the user a trigger so that the user might indicate that they were, in fact, on task (i.e. “I was on task”, or “Oops, I got distracted” trigger). However, given that the BCI commands of our system are generated every 100 ms or so, and that it takes approximately 500 ms for a participant to consciously decide to and actuate a trigger (Wegner, 2002, p. 57), we would first have to establish a method of synchronizing the trigger to the generated commands. One possibility would be to generate the trigger from the EEG signals themselves using the peak of the lateralized readiness potential (Wegner, 2002, p.50). However, we would still need to backtrack and assign the trigger to a previously executed command. The trigger tag on a particular move command could inform us whether or not those particular EEG commands should be used for training or not.

Another possibility would be to extend the decision making time from the current 124 ms to say, 500 ms. That is, instead of using 16 data points to generate a command, use 64 ( $7.8 * 64 = 499$  ms). This would facilitate the synchronization of a trigger to the command because they could occur roughly in the same time window.

Yet another possibility would be to assume a particular trigger value applies to say, the previous 5 - 10 commands. This would increase the likelihood that we could identify EEG signals that were associated with the task, and not some other fleeting thought.

We have demonstrated that averaging signals from several consecutive data packets dramatically improves the performance of our ANN. Implementing this approach in conjunction with a trigger as discussed above could further ensure the EEG data being used for training is not corrupted by EEG signals not related to the intended instruction.

In any of the above implementations, increasing the likelihood that good EEG patterns are used for training would greatly simplify the learning and generalization processes. Time did not permit these different approaches to be explored.

## CHAPTER NINE

### SUMMARY AND CONCLUSIONS.

#### **Transfer of motor learning.**

In chapters 1-7, we attempted to better understand the transfer of motor learning. We are fairly confident that we have demonstrated that the transfer of motor learning has more to do with the utilization of shared neural structures during both imagery and actual motor execution than with general arousal, attention, and other cognitive processes. Since more participants in the abstract group were able to learn the task than those in the embodied group, we are fairly certain that participants in the abstract group were at least as motivated and engaged in the task as those in the embodied group. However, it was the embodied group that showed learning transfer, not the abstract group. This undermines the notion that learning transfer has more to do with arousal, motivation, attention, and other physiological and psychological factors and bolsters the notion that transfer is due to shared neural structures between imagination and physical performance. However, we were not able to address the reasons that other psychological and physiological factors were considered in the first place. That is, we still have not addressed why there is transference of motor learning to non-homologous musculature. If we accept that transference has to do with shared neural infrastructure, then perhaps transference of motor learning to non-homologous motor systems also has to do with shared neural structures.

Wang and Sainburg, (2006) demonstrated that when visuo-motor execution training occurs in the ipsilateral workspace, transfer is symmetrical from dominant to non-dominant arms and visa-versa. However, when the visuo-motor task occurs across the midline, transfer is not symmetrical. Transfer of initial direction information only occurs from the

nondominant to dominant arm, whereas information about final position only transfers from the dominant to the nondominant arm. It seems that mirror image activation along with inhibition across the midline must be taking place during motor execution. Although Wang and Sainburg used actual physical practice, it remains to be seen if the same applies to mental imagery. It may be that both imagery and motor execution activate mirrored structures in the contralateral hemisphere, but the imagery does not provide the requisite contralateral inhibition required during actual motor execution. This might explain the Amemiya et al's. (2010) finding that motor execution did not transfer to the non-dominant side, whereas motor imagery did (see also Kirsch & Hoffmann, 2010).

It may be that shared neural infrastructure does fully explain motor learning transfer per se, but that transfer of motor learning to non-homologous motor structures involves more complex patterns of excitation and inhibition that differ during imagery and motor execution. Mirror image activations could, therefore, also offer an explanation for motor learning transfer to non-homologous motor systems.

## **Artificial Neural Networks for Processing EEG Data.**

In Chapter 8, we described a way to map EEG signals generated with different types of imagery into machine commands. We demonstrated that we can use fast Fourier transforms of EEG data over short time windows, and use the resulting power matrices as inputs to an artificial neural network which can learn the mapping from EEG signals to desired commands using a simple error back-propagation algorithm.

We also stressed the importance of ensuring that bad examples are filtered out of the training samples, and that data averaging is a viable method of addressing this issue. We have suggested several alternative ways to ensure the quality of the training sets, although we have not implemented them at this time. It is important to note that others have suggested that introducing errors into the training set may actually improve performance (Grossman & Lapedes, 1994). However, their method of introducing errors into the data is appropriate only when there is paucity of data. Imagine over-fitting a curve to a few sparse data points. A perfect fit may produce a model that is a horrible predictor of the data in general. In our situation, with examples generated around every 124 ms or so, lack of examples was not a concern.

The excitement generated over the possibility of controlling a machine with one's thoughts made it easy to get volunteers for our study. However, many hurdles have to be jumped before EEG-BCIs become more mainstream. The use of wet and often messy electrodes and better signal filtering are but a few obstacles. Until dry electrodes become more available, and the technology easier to use, it is unlikely that EEG-BCI control will become mainstream (Nijholt & Tan, 2008). Some companies and researchers are already producing dry electrode EEG devices (G.tec Medical Engineering, Inc., Taheri et al., 1994;

Gargiulo et al. 2008), so it will not be long before EEG-BCI technology becomes more ubiquitous.

We have demonstrated a relatively simple open source method for mapping EEG signals into machine commands. In addition we have demonstrated that different types of imagery (abstract versus embodied) may be best for different types of disabilities. That is, ALS patients may be better off learning abstract imaging for EEG-BCI control, while stroke patients may be better off learning embodied control. We suggest that this open source method of mapping EEG signals to machine commands will foster the development and proliferation of EEG-BCI technology for all and facilitate superior EEG control performance for a large variety of individuals.

### **Take Home Messages.**

#### ***Part 1.***

We utilized an EEG Brain Computer Interface (BCI) to explore the transfer of motor learning from imagery to motor execution of a task. We demonstrated that EEG-BCI control is generally easier to learn using abstract imagery than embodied imagery, but motor learning transfer to motor performance can only be expected from embodied imagery. We take this as evidence to suggest that the transfer of motor learning from imagery to the motor execution is the result of shared neural infrastructure between embodied imagery and actual motor execution.

Because motor learning transfer from imagery to motor execution can only be expected with embodied imagery, embodied imagery is recommended if EEG-BCIs are being used for rehabilitation and training aimed at acquiring or reacquiring motor skills.



However, when one is not concerned with coupling EEG-BCI control with specific motor processes (e.g. for those with degenerative diseases where there is currently no hope of neuromuscular recovery such as ALS), abstract imagery is recommended, because it is easier to learn. Of course when possible, physical motor execution practice is preferred.

### ***Part 2.***

EEG-BCI control can be achieved using a variety of methods. We introduce the use of an artificial neural network that utilizes the averaged time-frequency-power spectrograms of the EEG signals over time and have shown that it is as good as or better than Emotiv's proprietary method. In addition our method of mapping EEG signals into computer commands can be configured so that it is adaptive to better match individual predispositions and adjust to changing neural signatures as skill learning progresses.

## REFERENCES

1. Adams, J. A. (1987). Historical review and appraisal of research on the learning, retention, and transfer of human motor skills. *Psychological Bulletin*, 101(1), 41-74.
2. Amemiya, K., Ishizu, T., Ayabe, T., & Kojima, S. (2010). Effects of motor imagery on intermanual transfer: A near-infrared spectroscopy and behavioral study. *Brain Research*, 1343, 93-103.
3. Bradberry, T.J., Gentili, R.J., and Contreras-Vidal, J.L. (2011). Fast attainment of computer cursor control with noninvasively acquired brain signals. *Journal of Neural Engineering*. 8, 1-9.
4. Butler, A. J. & Page, S. J. (2006). Mental practice with motor imagery: Evidence for motor recovery and cortical reorganization after stroke. *Archives of Physical Medicine and Rehabilitation*, 8 (2), 1-17.
5. Carey, J. R. (1990). Manual stretch: Effect on finger movement control and force control in stroke subjects with spastic extrinsic finger flexor muscles. *Archives of Physical Medicine Rehabilitation*, 71, 888-894.
6. Carey, J. R., Kimberley, T. J., Lewis, S. M., Auerbach, E. J., Dorsey, L., Rundquist, P., & Ugurbil, K. (2002). Analysis of fMRI and finger tracking training in subjects with chronic stroke. *Brain*, 125(4), 773-778.
7. Cerna, M. & Harvey, A. F. (2000). The fundamentals of FFT-based signal analysis and measurement. *National Instruments Application*, Note 041. Retrieved March 1, 2013, from <http://www.lumerink.com/courses/ece697/docs/Papers/The%20Fundamentals%20of%20FFT-Based%20Signal%20Analysis%20and%20Measurements.pdf>
8. Danilo P. M. & Chambers, J. A. (2000). Towards the optimal learning rate for backpropagation. *Neural Processing Letters*, 11(1), 1370-4621
9. Debarnot, U., Castellani, E., Valenza, G., Sebastiani, L., & Guillot, A. (2011). Daytime naps improve motor imagery learning. *Cognitive, Affective, & Behavioral Neuroscience*, 11(4), 541-550.
10. Debarnot, U., Louis, M., Collet, C., & Guillot, A. (2011). How does motor imagery speed affect motor performance times? Evaluating the effects of task specificity. *Cognitive, Affective, & Behavioral Neuroscience*, 25(4), 536-540.

11. Decety, J. (1996). Do imagined actions share the same neural substrate? *Cognitive Brain Research*, 3, 87-93.
12. Deora, D., & Bajaj, N. (2012, December). Indian sign language recognition. In *Emerging Technology Trends in Electronics, Communication and Networking (ET2ECN), 2012 1st International Conference on* (pp. 1-5). IEEE.
13. Driemeyer, J., Boyke, J., Gaser, C., Buchel, C., and May, A. (2008). Changes in gray matter induced by learning-revisited. *PLoS One*, 3(7), 1-5.
14. Elman, J. L., Bates, E. A., Johnson, M. H., Karmiloff-Smith, A., Parisi, D., & Plunkett, K. (1997). Rethinking innateness: A connectionist perspective on development, (pp. 81). Cambridge, MA: MIT Press.
15. Estrera, R. M., Romana, C. L. C. S., & Maravillas, E.A. (2012). Face recognition using back-propagation neural networks and openCV®. *IAMURE International Journal of Mathematics, Engineering & Technology*, 4(1).
16. Filimon, F., Hagler, D. J., & Sereno, M. I. (2004). Overlapping neural substrates for executed, observed, and imagined movements. *Presented at Cognitive Neuroscience Society Annual Meeting. San Francisco*. April 18-20, 2004. "Filimon et al. 2004CNS.pdf", Retrieved July 6, 2011 from <http://kamares.ucsd.edu/cgi-bin/wrap/ffilimon/>.
17. Ehrsson, H. H., Geyer, S. & Naito, E. (2003). Imagery of voluntary movement of fingers, toes, and tongue activates corresponding body-part-specific motor representations. *Journal of Neurophysiology*, 90, 3304–3316.
18. Gargiulo, G.; Bifulco, P.; Calvo, R.A.; Cesarelli, M.; Jin, C.; van Schaik, A. (2008). A mobile EEG system with dry electrodes, *IEEE Biomedical Circuits and Systems Conference, 2008. November*. 273-276.
19. Gentili, R., Han, C. H., Schweighofer, N., & Papaxanthis, C. (2010). Motor learning without doing: Trial-by-trial improvement in motor performance during mental training. *Journal of Neurophysiology*, 104, 774–783.
20. Gravetter, F. J. & Wallnau, L. B. (2000). Statistics for behavioral sciences. Instructor's Edition. (5<sup>th</sup> ed.). Belmont, CA. Wadsworth Thompson Learning, 349 -350.

21. Gravetter, F. J. & Wallnau, L. B. (2011). *Essentials of Statistics for the Behavioral Sciences*. (7<sup>th</sup> Ed.). Belmont, CA. Wadsworth Cengage Learning, 396 -399.
22. Grossman, T. & Lapedes, A. (1994). Use of Bad Training Data for Better Predictions. Santa Fe Institute:SFI Working Paper. 1995-02-019
23. Haier, R.J., Siegel, B.V. Jr., MacLachlan, A., Soderling, E., Lottenberg, S., & Buchsbaum, M.S. (1992). Regional glucose metabolic changes after learning a complex visuospatial/motor task: a positron emission tomographic study. *Brain Research*, 570, (1-2), 134-143.
24. Hall, C. R., Mack, D. E., Paivio, A., & Hausenblas, H. A. (1998). Imagery use by athletes: Development of the sport imagery questionnaire. *International Journal of Sport Psychology*, 29, 73-89.
25. Hunter, D., Yu, H., Pukish, M. S., Kolbusz, J., & Wilamowski, B. M. (2012). Selection of proper neural network sizes and architectures – A comparative study. *IEEE Transactions on Industrial Informatics*, 8(2) 228 -240.
26. Jeannerod, M. (2001). Neural simulation of action: a unifying mechanism for motor cognition. *NeuroImage*, 14(1 Pt 2), S103-9.
27. Johnson, S. H. (2000). Imagining the impossible: intact motor representations in hemiplegics. *Neuroreport*, 11(4), 729-732.
28. Kirsch, W. & Hoffmann, J. (2010). Asymmetrical intermanual transfer of learning in a sensorimotor task. *Experimental Brain Research*, 202, 927-934.
29. Kostov, A., & Polak, M. (2000). Parallel man-machine training in development of EEG-based cursor control. *IEEE Transactions on Rehabilitation Engineering*, 8(2), 203-205.
30. Lamm, C., Windischberger, C., Moser, E., & Bauer, H. (2007). The functional role of dorso-lateral premotor cortex during mental rotation: an event-related fMRI study separating cognitive processing steps using a novel task paradigm. *NeuroImage*, 36(4), 1374-86.
31. Lippmann, R. P. (1987). An Introduction to computing with neural nets. *IEEE ASSP Magazine*, 4(2), 4 - 22.

32. Lehmann, D., Pascual-Marqui, R. D., Strik, W. K., & Koenig, T. (2010). Core networks for visual-concrete and abstract thought content: A brain electric microstate analysis. *Neuroimage*, 49(1), 1073–1079.
33. Miller, K. J., Schalk, G., Fetz, E. E., den Nijs, M., Ojemann, J. D., & Rao, R. P. N. (2010). Cortical activity during motor execution, motor imagery, and imagery-based online feedback. *Proceedings of the National Academy of Sciences (PNAS)*, 107(9), 4430–4435.
34. Nijholt, A., Tan, D., Pfurtscheller, G., Brunner, C., Millan, J. R., Allison, B., et al. (2008). Brain-computer interfacing for intelligent systems. *IEEE Intelligent Systems*, 23(3), 72–79.
35. Page, S. J., Dunning, K., Hermann, V., Leonard, A. & Levine, P. (2011). Longer versus shorter mental practice sessions for affected upper extremity movement after stroke: a randomized controlled trial. *Clinical Rehabilitation*, 25(7), 627-637.
36. Paivio A. (1985). Cognitive and motivational functions of imagery in human performance. *Canadian Journal of Applied Sport Sciences*, 10(4), 22-28.
37. Perry, H. M. (1939). Relative efficiency of actual and imaginary practice in five selected tasks. *Archives of Psychology*, 243, 3-76.
38. Ranganathan V. K., Siemionow V., Liu J. Z., Sahgal V., & Yue G. H. (2004). From mental power to muscle power—gaining strength by using the mind. *Neuropsychologia*, 42, 944–956.
39. Reiser, M., Busch, D., & Munzert, J. (2011). Strength gains by motor imagery with different ratios of physical to mental gains. *Frontiers in Psychology*, 2, 1-8.
40. Riva, N., Falini, A., Inuggi, A., Gonzales-Rosa, J. J., Amadio, S., Cerri, F., et al. (2012). Cortical activation to voluntary movement in amyotrophic lateral sclerosis is related to corticospinal damage: electrophysiological evidence. *Clinical Neurophysiology*. 123(8), 1586-1592.
41. Rumelhart, D. E., Hinton, G. E., and Williams, R. J. (1986). “Learning Internal Representation by Error Propagation”. In D.E. Rumelhardt, J. L. McClelland, and the PDP Research Group, “Parallel Distributed Processing”, (Vols. 1-2, Vol. 1). (pp. 318-362). Cambridge, MA: MIT Press.

42. Schnitzler, A., Salenius, S., Salmelin R., Jousmaki, V., & Hari, R. (1997). Involvement of primary motor cortex in motor imagery: A neuromagnetic study. *Neuroimage*, 6, 201–208.
43. Silvoni, S., Ramos-Murguialday, A., Cavinato, M., Volpato, C., Cisotto, G., Turolla, A., et al. (2011). Brain-computer interface in stroke: a review of progress. *Clinical EEG and Neuroscience*, 42(4), 245-252.
44. Silvoni, S., Ramos-Murguialday, A., Cavinato, M., Volpato, C., Cisotto, G., Turolla, A., et al. (2009). P300-based brain–computer interface communication: evaluation and follow-up in amyotrophic lateral sclerosis. *Frontiers in Neuroscience*, 3, 1-12.
45. Singh, A. (2012). Prosthetic Hand Control. *International Journal of Engineering Research and Applications (IJERA)*. 2(6),311-339.
46. Stanton, B. R., Williams, V. C., Leigh, P. N., Williams, S. C. R., Blain, C. R. V., Giampietro, V. P., & Simmons, A. (2007). Cortical activation during motor imagery is reduced in amyotrophic lateral sclerosis. *Brain Research*, 1172, 145-151.
47. Ste-Marie, D. M., & Cumming, J. L. (2001). The Cognitive and Motivational Effects of Imagery Training: A matter of Perspective. *The Sport Psychologist*, 15, 276–288.
48. Stoddard, J., & Vaid, J. (1996). Asymmetries in intermanual transfer of maze learning in right-and left-handed adults. *Neuropsychologia*, 34(6), 605-608.
49. Taheri, B.A., Knight, R.T., Smith, R.L. (1994). A dry electrode for EEG recording. *Electroencephalography and Clinical Neurophysiology*, 90(5), 376–383
50. Thorndike, E. L. & Woodworth, R. S. (1901). The influence of improvement in one mental function upon the efficiency of other functions. *Psychological Review*, 8, 247-261.
51. Vangheluwe, S., Puttemans V., Wenderoth, N., Van Baelen, M., & Swinnen, S. P. (2004). Inter- and intralimb transfer of a bimanual task: generalizability of limb dissociation. *Behavioural Brain Research*, 154(2), 535-547.

52. Van Mier, H. I., & Petersen, S. E. (2006). Intermanual transfer effects in sequential tactuomotor learning: evidence for effector independent coding. *Neuropsychologia*, *44*(6), 939–49.
53. Wang, J., & Sainburg, R. L. (2006). The symmetry of interlimb transfer depends on workspace locations. *Experimental Brain Research*, *170*(4), 464–71.
54. Wegner, Daniel M. (2002). *The Illusion of conscious will*. Cambridge, Massachusetts: The MIT press.
55. Wilamowski, B.M., & Yu, H. (2010). Neural Network Learning without Backpropagation. *IEEE Transactions on Neural Networks*. *21*(11). 1793–1803.
56. Yaguez, L., Nagel, D., Hoffman, H., Canavan, A. G. M., Wist, E., & Homberg, V. (1998). A mental route to motor learning: Improving trajectorial kinematics through imagery training. *Behavioural Brain Research*, *90*, 95–106.
57. Yaguez, L., Canavan, A. G. M., Lange, H. W., & Homberg, V. (1999). Motor learning by imagery is differentially affected in Parkinson's and Huntington's diseases. *Behavioural Brain Research*, *102*, 115–127.
58. Yasuda, Y., & Miyamura, M. (1983). Cross transfer effects of muscular training on blood flow in the ipsilateral and contralateral forearms. *European Journal of Applied Physiology*, *51*, 321–329.
59. Yin, Y. H.; Fan, Y. J. & Xu, L. D. (2012). EMG and EPP-integrated human-machine interface between the paralyzed and rehabilitation exoskeleton. *IEEE Transactions on Information Technology in Biomedicine*, *16* (4), 542-549.
60. Yue, G., Cole, K. J. (1992). Strength increases from the motor program: comparison of training with maximal voluntary and imagined muscle contractions. *Journal of Neurophysiology*, *67*(5), 1114-1123.

APPENDIX A  
EXACT BINOMIAL DISTRIBUTIONS



To determine the probability of throwing a coin that turns up heads exactly  $x$  times after 12 tosses with a fair coin ( $p=0.5$ ) we use the probability function where  $p = 0.5$ ,  $N = 12$ , is shown in Figure A1:

$$P(x = k) = \left( \frac{N!}{x!(N-x)!} p^x (1-p)^{(N-x)} \right)$$

(13)

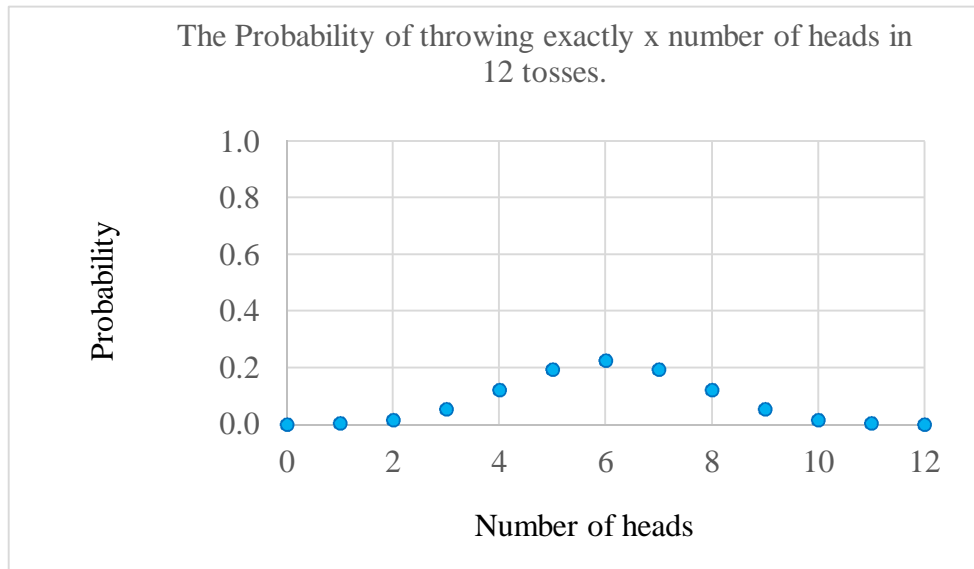


*Figure A1.* Probabilities with a fair coin. The probability of throwing exactly  $x$  number of heads in 12 tosses with a fair coin ( $p=0.5$ ).

The cumulative probability that we throw  $x$  or more heads in 12 tosses with a fair coin ( $p=0.5$ ), shown in Figure A2, is given by the exact binomial distribution:

$$P(x \geq k) = \sum_{x=k}^N \left( \frac{N!}{x!(N-x)!} p^x (1-p)^{(N-x)} \right)$$

(14)

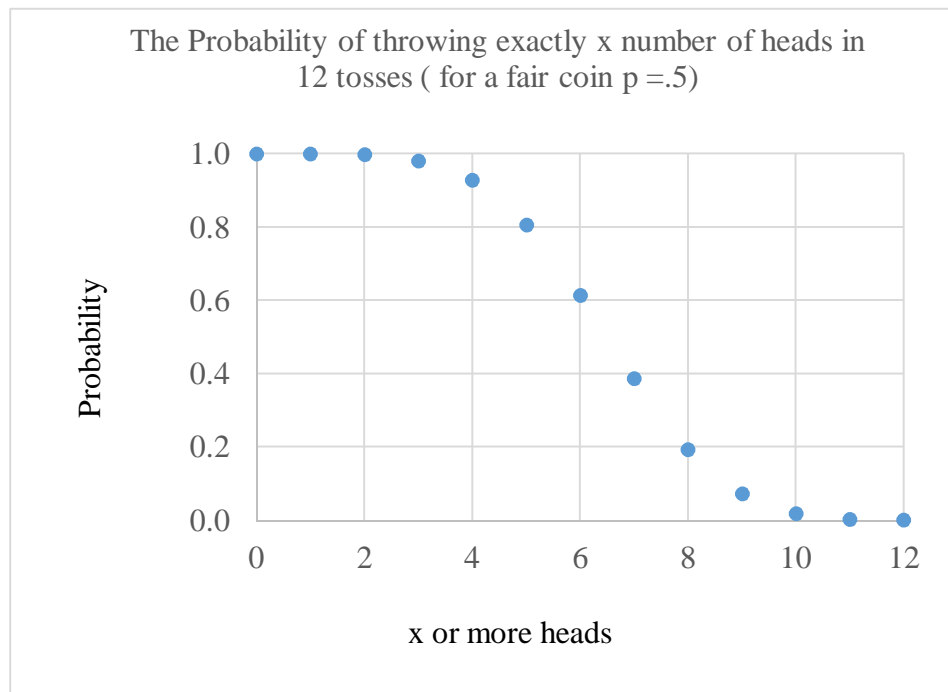
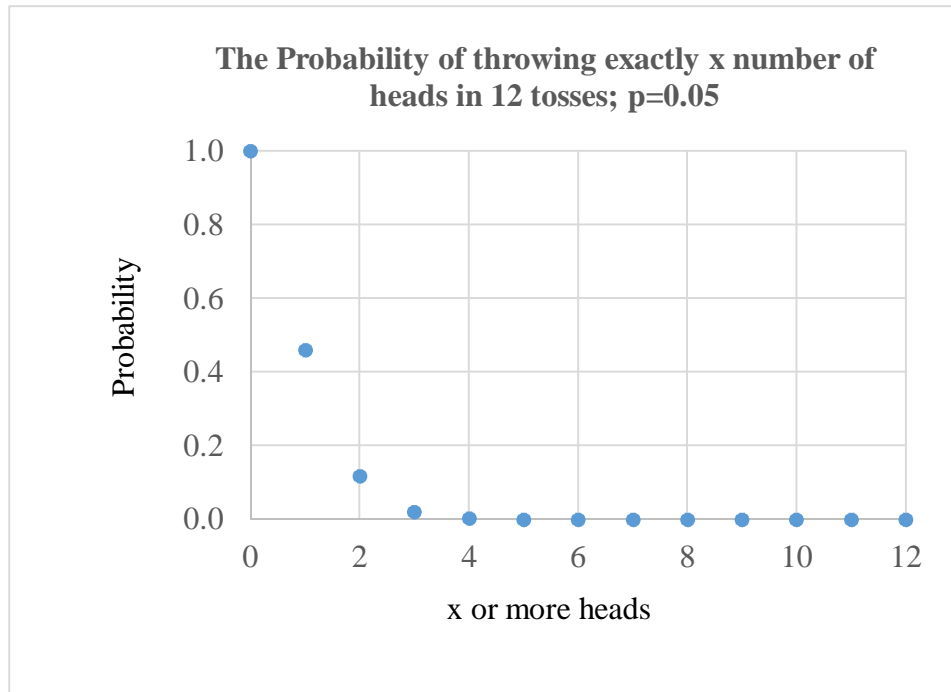


Figure A2. Cumulative probabilities with a fair coin. The cumulative probability of throwing  $x$  or more heads in 12 tosses with a fair coin ( $p=0.5$ ).

If however, our coin is not fair, we simply change the  $p$  value in the cumulative probability function above to, say 0.05. The cumulative probability of throwing  $x$  or more heads in 12 tosses with an unfair coin ( $p=0.05$ ) is shown in Figure A3.



*Figure A3.* Cumulative probabilities with an unfair coin. The cumulative probability of throwing  $x$  or more heads in 12 tosses with an unfair coin ( $p=0.05$ ).

The above is the rationale for using the cumulative probability distribution to determine the likelihood that the number of participants who improved after practice occurred by chance or as a result of practice. We simply changed coin to participants, and the unfair coin has the  $p=0.05$  probability that the participants did not get better merely by chance alone.

## BIOGRAPHICAL SKETCH

My meandering route to a cognitive psychology PhD. began with a background in engineering. After receiving my first master's degree in agricultural engineering, I worked for University of Georgia as a research engineer. After a two years, it was time for a new adventure. I spent time traveling, exploring, and soul searching before deciding to go back to school and enrolling at Georgia Institute of Technology. After completing a second master's in mechanical engineering and robotics, I worked for Intel Corporation. For eight years I developed manufacturing technology, automated factories, and helped launch new products. During my time at Intel, I realized that traditional engineering approaches were sometimes inferior to biologically inspired approaches for solving certain problems. Recognition, for instance, is so easy for us, yet so difficult to program. This prompted my interest in psychology and neuroscience. Intrigued, I went back to school at Arizona State University, and thanks to the encouragement of Dr. Presson, finally joined the cognitive psychology program. I found elements of applied psychology to be most interesting. For my master's, I worked with Drs. Sugar and McBeath on wearable robotics for stroke rehabilitation. Then I met Dr. Helms Tillery who introduced me to neural prosthetics. Much of what I learned working for Dr. Helms Tillery at the sensorimotor research group enabled me to complete this current project in EEG-BCI for machine control. I hope to continue multidisciplinary applied research in psychology, neuroscience and robotics in the future.